

1 *Original Research Article*

2 **Synthesis, Spectral and Thermal Characterization**  
3 **with Antimicrobial Activity Studies on Some Metal**  
4 **Complexes Containing Schiff Base Ligand**  
5  
6  
7

8 Abstract

9 Some metal complexes of Ni(II), Zn(II), Mn(II), Sn(II), Co(II) and Cd(II) ions were  
10 synthesized with three different synthesized Schiff base ligands. The ligands and metal  
11 complexes were isolated in solid state from the reaction medium and characterized by molar  
12 conductivity measurement, magnetic susceptibility, Infrared, electronic spectral, thermal  
13 analysis and some physical measurements. The overall reactions were monitored by TLC  
14 analysis. Molar conductance study have shown that all the complexes were non electrolytic in  
15 nature. FTIR studies suggested that Schiff bases act as deprotonated bidentate ligands and  
16 metal ions are attached with the ligands through N, O/S coordinating sites during  
17 complexation reaction. Magnetic susceptibility data coupled with electronic spectra revealed  
18 that Zn(II), Mn(II), Sn(II), and Cd(II) complexes have tetrahedral, Ni(II) complexes has square  
19 planer and Co(II) complexes has octahedral geometry. Thermal analysis (TGA and DTG) data  
20 showed the possible degradation pathway of the complexes and also indicated that most of  
21 the complexes were thermally stable up to 200<sup>0</sup>C. The Schiff bases and their metal complexes  
22 have been found moderate to strong antimicrobial activity.

23 Keywords: Schiff Base, Thiosemicarbazide, TGA, DTG, Antimicrobial activity

24 **1 INTRODUCTION**

25 Multidentate ligands are extensively used for the preparation of metal complexes with  
26 interesting properties [1-5]. Among these ligands, Schiff bases containing nitrogen and  
27 phenolic oxygen donor atoms are of considerable interest due to their potential application in  
28 catalysis, medicine and material science [6-9]. Transition metal complexes of these ligands  
29 exhibit varying configurations, structural liability and sensitivity to molecular environments.  
30 The central metal ions in these complexes act as active sites for pharmacological agent.  
31 This feature is employed for modeling active sites in biological systems.

32 Thiosemicarbazones obtained by the condensation reaction of thiosemicarbazide and  
33 different aldehydes or ketones are important chemicals due to their broad profile of  
34 pharmacological activity. The transition metal complexes of thiosemicarbazone are also  
35 played important role in antimicrobial, antitumor and anticancer activities.

36 Therefore, in view of our interest in synthesis of new Schiff base complexes, which might  
37 find application as pharmacological and as luminescence probes, we have synthesized and  
38 characterized new transition metal complexes of Schiff bases formed by the condensation  
39 reaction of different aldehydes and amino acids. The results of our studies are presented in  
40 this article.

## 41 **2. Experimental**

### 42 **2.1 Materials and Methods**

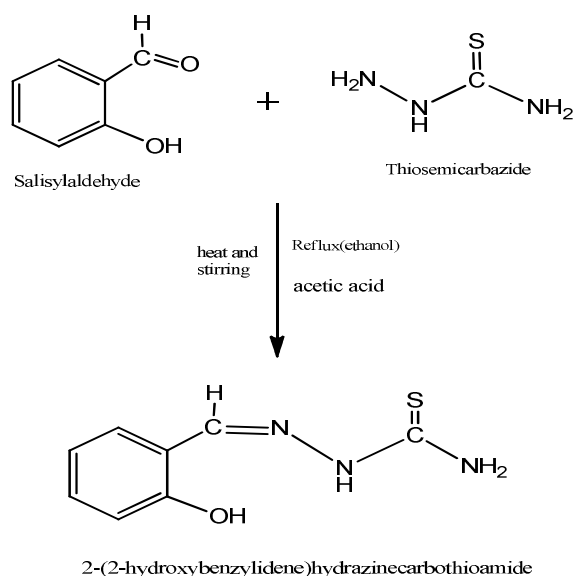
43 All chemicals and solvents used were of Analar grade. All metal(II) salts were used as  
44 chloride and sulphate. The solvents such as Ethanol, methanol, chloroform, Diethyl ether,  
45 petroleum ether, DMSO (dimethyl sulfoxide) and acetonitrile were purified by standard  
46 procedure. The melting point or the decomposition temperature of all the prepared ligand and  
47 metal complexes were observed in an electro thermal melting point apparatus model No.  
48 AZ6512. Vibrational spectra (IR) were recorded with a NICOLET 310, FTIR  
49 spectrophotometer, Belgium, in the range  $4000-225\text{ cm}^{-1}$  with a KBr disc as reference. UV-  
50 Visible spectra of the complexes in DMSO ( $0.5 \times 10^{-3}\text{ M}$ ) were recorded in the region 200-800  
51 nm on a Thermolectron Nicolet evolution 300 UV-Visible spectrophotometer. The  
52 SHERWOOD SCIENTIFIC Magnetic Susceptibility Balance that following the Gouy  
53 Method were used to measure the magnetic moment of the solid complexes. The electrical  
54 conductance measurements were made at room temperature in freshly prepared aqueous  
55 solution ( $10^{-3}\text{ M}$ ) and in DMSO using a WPACM35 conductivity meter and a dip-cell with a  
56 platinum electrode. some conductivity were also measured in PTI-18 Digital conductivity  
57 meter. The purity of the ligand and metal complexes were tested by Thin Layer  
58 Chromatography (TLC).

59

#### 60 **2.1 Synthesis of Schiff base Ligand $\text{C}_8\text{H}_9\text{ON}_3\text{S}$ (L<sup>1</sup>)**

61 The ligand was prepared by condensation reaction of 20 mmole of salicylaldehyde (1.048ml)  
62 with 20 mmole (1.82gm) of thiosemicarbazide in a clean round bottomed flask.  
63 Salicylaldehyde was dissolved in 20ml ethanol and thiosemicarbazide was dissolved in hot

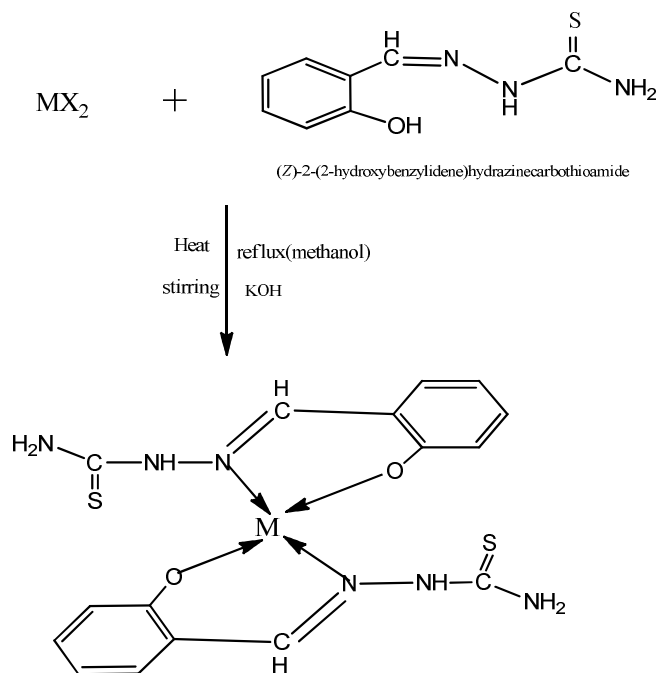
64 ethanol with water. The solutions were mixed and refluxed for 3-4 hours. On cooling off  
 65 white colored product was formed which was washed with ethanol, acetone, and diethyl ether  
 66 and dried in vacuum desiccators over anhydrous  $\text{CaCl}_2$ . The purity of ligand was tested by  
 67 TLC using different solvents. The product was found to be soluble in methanol, chloroform  
 68 and DMSO. It provided 80% yield at  $34^\circ\text{C}$ . The target Schiff base was synthesized according  
 69 to Figure-1.



70

71 Figure-1: Synthesis pathway of Schiff base ligand  $\text{C}_{14}\text{H}_{11}\text{O}_3\text{N}$  ( $\text{L}^1$ )72 **2.3 Synthesis of Metal Complexes Using Schiff Base Ligand  $\text{C}_{14}\text{H}_{11}\text{O}_3\text{N}$  ( $\text{L}^1$ )**

73 The synthesized complexes have the general formula  $[\text{M}(\text{SB})_2]$ ; where  $\text{M} = \text{Zn}(\text{II}), \text{Ni}(\text{II})$  and  
 74  $\text{Mn}(\text{II})$  and  $\text{SB} =$  synthesized Schiff base ligand (Fig-3). During complexation reaction, 15ml  
 75 methanolic solution of Zinc(II) sulphate (0.2875g, 1mmol)/ Ni(II) chloride hexahydrate  
 76 (0.238g, 1mmol)/ Manganese(II) chloride tetrahydrate (0.198g, 1mmol) was taken in a two  
 77 necked round bottom flask and kept on a magnetic stirring. A methanolic solution (20 mL) of  
 78 prepared Schiff base ligand (0.390g, 2mmol) was added drop wise and a methanolic solution  
 79 (10mL) of KOH (0.1122g, 1mmol) was added slowly then the resultant mixture was heated  
 80 with constant stirring on a magnetic stirrer for 4-5 hours. On cooling colored solid product  
 81 was formed which was washed with methanol, acetone, ether and dried in vacuum over  
 82 anhydrous  $\text{CaCl}_2$ . The reaction was monitored by TLC using petroleum ether, toluene, ethyl  
 83 acetate and methanol as solvent. The common structure of metal complexes has shown in  
 84 (Figure-2-6).



85

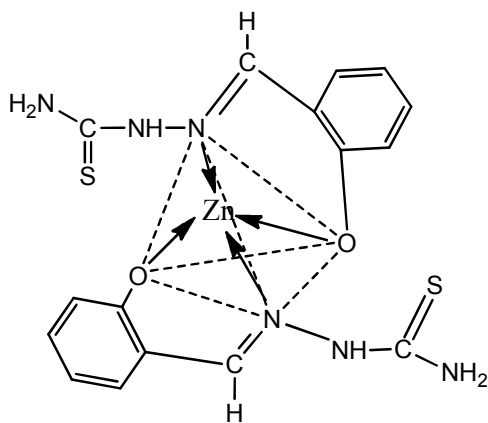
Figure-2: Synthesis pathway of Schiff Base Ligand ( $L^2$ ) Metal Complexes

86

Where,  $M=Zn(II)$ ,  $Ni(II)$ ,  $Mn(II)$ , and  $Sn(II)$  ions and  $X=Cl^-,SO_4^{2-}$  ions

87

88

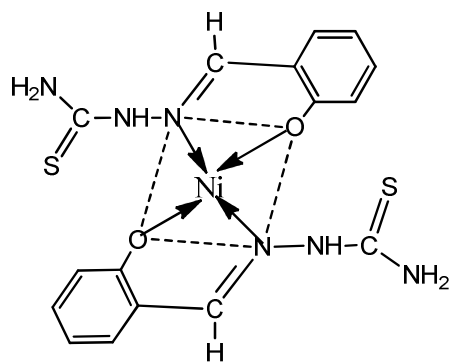


89

Figure-3: Structure of  $[C_{16}H_{16}ZnO_2N_6S_2]$  Comp

90

91

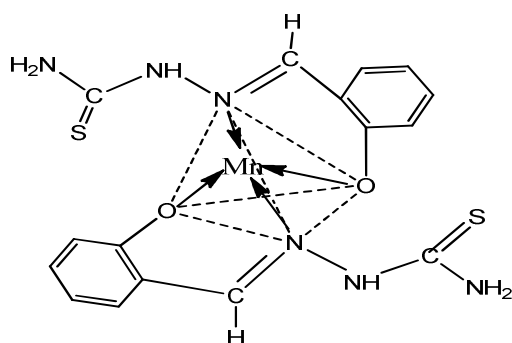


92

93

Figure-4: Structure of  $[C_{16}H_{16}NiO_2N_6S_2]$  Complex

94

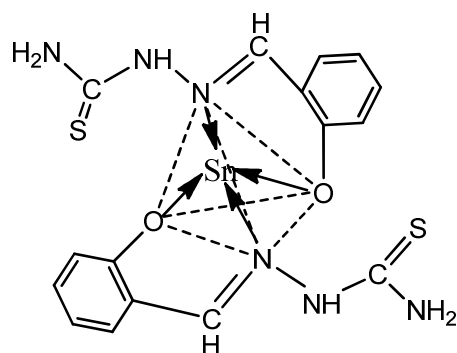


95

96

Figure-5: Structure of  $[C_{16}H_{16}MnO_2N_6S_2]$  Complex

97



98

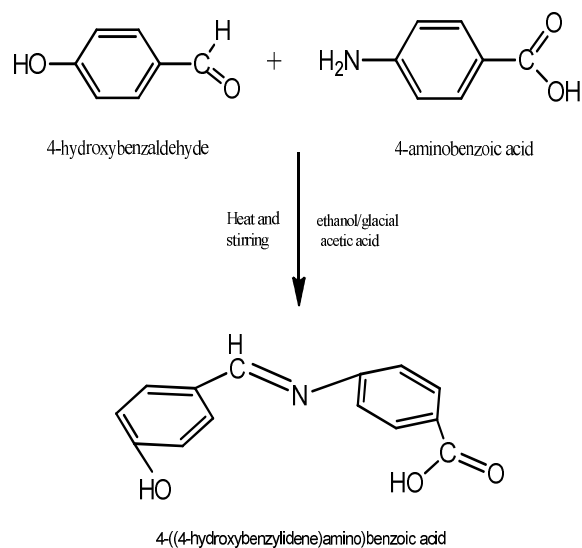
99

Figure-6: Structure of  $[C_{16}H_{16}SnO_2N_6S_2]$  Complex

#### 100 2.4 Synthesis of Schiff Base Ligand $C_{14}H_{11}O_3N$ ( $L^2$ )

101 4-hydroxy benzaldehyde (2.44g, 20 mmol) dissolved in absolute ethanol (20-25 mL) was  
 102 added drop wise to a constant stirring solution of 4-aminobenzoic acid(2.76 g, 20 mmol) in  
 103 30 mL ethanol and 2 mL of conc. glacial acetic acid was added slowly. Then the mixture  
 104 was refluxed for (4-5)h. On cooling, a solid yellow product was formed which was filtered,

105 washed with ethanol and diethyl ether and dried in vacuum over anhydrous  $\text{CaCl}_2$ . The  
 106 reaction was monitored by TLC using petroleum ether, ethyl acetate, toluene and methanol  
 107 solvents. The product was found to be soluble in methanol, chloroform and DMSO. It  
 108 provided 65% yield at  $34^\circ\text{C}$ . The target Schiff base was synthesized according to Figure-7.

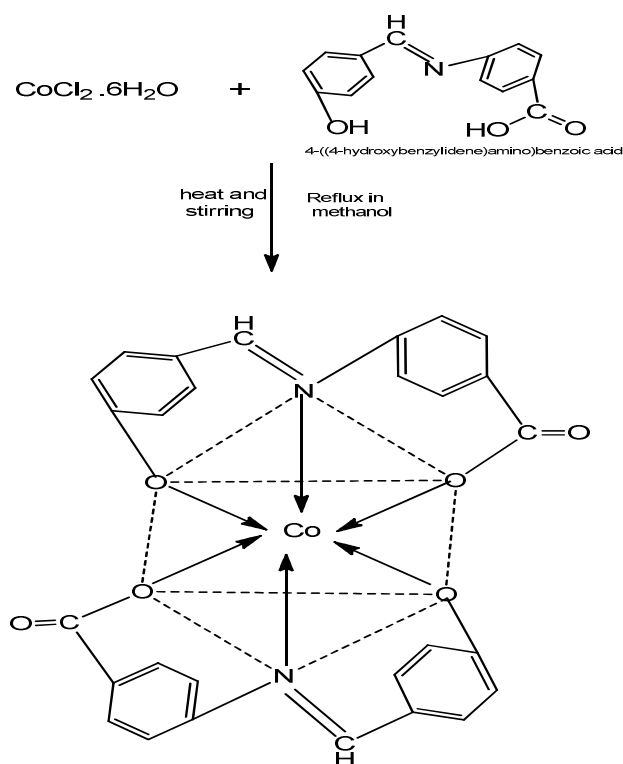


109

110 Figure-7: Synthesis pathway of Schiff base ligand  $\text{C}_{14}\text{H}_{11}\text{O}_3\text{N}$  ( $\text{L}^2$ )

### 111 2.5 Synthesis of Metal Complex Using Schiff Base Ligand ( $\text{L}^2$ )

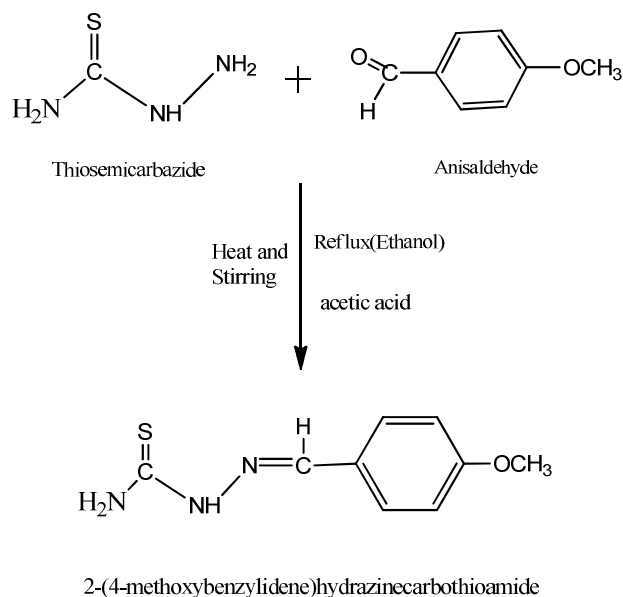
112 The complex was prepared in 1:2 molar ratio (metal : ligand). A methanolic solution (20  
 113 mL) of cobalt(II) chloride hexahydrate (0.24 g, 1 mmol) was taken in a two necked round  
 114 bottom flask and kept on magnetic stirring and a methanolic solution (20 mL) of prepared  
 115 Schiff base ligand (0.483 g, 2 mol) was added drop wise and stirred with heating for 4-5h. On  
 116 cooling, precipitate was formed which was filtered, washed with ethanol, acetone, and diethyl  
 117 ether and dried in vacuum desiccators over anhydrous  $\text{CaCl}_2$ . The purity of complex was  
 118 tested by TLC using different solvents. The complex was soluble in DMSO with heat. The  
 119 proposed structure of complex was shown in (Figure-8).



120

121 Figure-8: Synthesis pathway of Co(II) complex with Schiff Base Ligand ( $L^2$ )122 **2.6 Synthesis of Schiff base Ligand  $C_9H_{11}N_3OS$  ( $L^3$ )**

123 To a stirring solution of thiosemicarbazide (0.91 gm, 10 mmol) dissolved in 20mL of ethanol  
 124 with water, a solution of Anisaldehyde(1.22mL,10mmol) in 10mL ethanol was added drop wise.  
 125 After sometime 2ml of glacial acetic acid was added with the reaction mixture and the solution  
 126 was refluxed for 5-6 h and allowed to cool overnight in room temperature. The off white  
 127 product was filtered washed several times with ethanol and finally with diethyl ether and dried in  
 128 vacuum over anhydrous  $\text{CaCl}_2$ . The reaction was monitored by TLC using petroleum ether,  
 129 ethyl acetate, toluene and methanol solvents .The product was found to be soluble in methanol,  
 130 DMF and DMSO. It provided 62% yield. The Schiff base was synthesized according to  
 131 Figure-9.



132

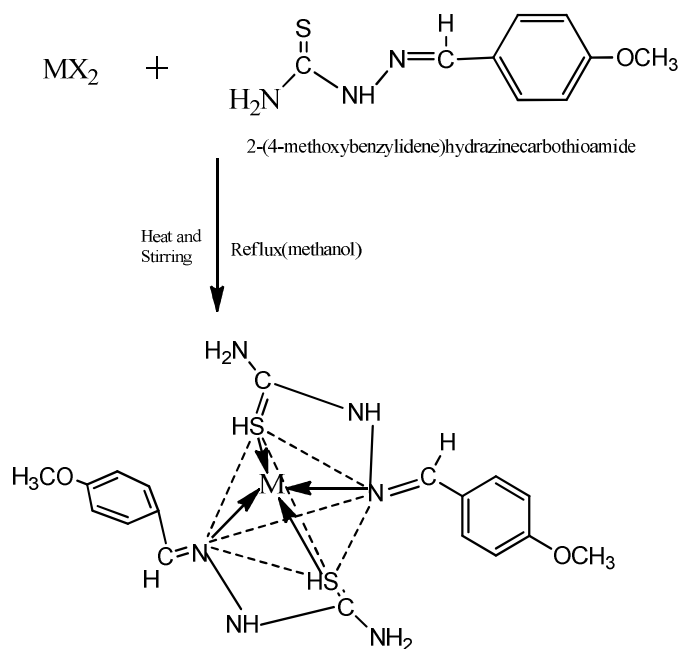
133

Figure-9: Synthesis pathway of Schiff base ligand  $C_9H_{11}N_3OS$  ( $L^3$ )

### 134 2.7 Synthesis of Metal Complex Using Schiff Base Ligand ( $L^3$ ):

135 The complex was prepared in 1:2 molar ratio (metal : ligand). Methanolic solution (20 mL) of  
 136 cadmium(II) chloride dihydrate (0.228g, 1mmol) was taken in a two necked round bottom  
 137 flask and kept on magnetic stirring. A methanolic solution (20 mL) of prepared Schiff base  
 138 ligand ( $L^3$ ) (0.418g, 2mmol) was added drop wise and stirred with heating for 4-5h. On  
 139 cooling, precipitate was formed which was filtered, washed with ethanol, acetone, and diethyl  
 140 ether and dried in vacuum desiccators over anhydrous  $CaCl_2$ . The reaction was monitored by  
 141 TLC using different solvents. The complex was soluble in DMSO with heat. The proposed  
 142 structure of complex was shown in (Figure-10).





143

144

Figure-10: Synthesis pathway of Schiff Base Ligand ( $L^4$ ) Metal Complex

145

Where,  $M=Cd(II)$  ions

146

**3. Characterization of the Ligands and Complexes**

147

The structures of the complexes were characterized by melting point, conductivity measurements, magnetic susceptibility, IR spectra and UV visible spectra [10] analysis. The purity of the ligands and metal complexes was monitored by Thin Layer Chromatography (TLC). The ligands and complexes are characterized below by these methods.

150

151

**3.1 Melting point**

152

Melting point gives an approximate idea about the nature of the complexes and can suggest whether it is covalent or ionic [11]. The melting point of all the synthesized ligands and complexes are shown in Table-1.

153

154

**Table-1:** Physical characteristics and analytical data of ligands and complexes

Compound/Empirical Formula	Formula Weight	Color	Yield(%)	Melting Point/ Decomposition temp.( $^{\circ}C$ )

155

156

157

Ligand (L <sup>1</sup> ) C <sub>8</sub> H <sub>9</sub> ON <sub>3</sub> S	195	off white	80 %	215 <sup>0</sup> C - 217 <sup>0</sup> C
[Zn (L <sup>1</sup> ) <sub>2</sub> ] .2H <sub>2</sub> O [ZnC <sub>16</sub> H <sub>16</sub> O <sub>2</sub> N <sub>6</sub> S <sub>2</sub> ].2H <sub>2</sub> O	491.38	cream color	67 %	above 300 <sup>0</sup> C
[Ni (L <sup>1</sup> ) <sub>2</sub> ].H <sub>2</sub> O [NiC <sub>16</sub> H <sub>16</sub> O <sub>2</sub> N <sub>6</sub> S <sub>2</sub> ].H <sub>2</sub> O	466.93	yellow green	70 %	275 <sup>0</sup> C - 280 <sup>0</sup> C
[Mn (L <sup>1</sup> ) <sub>2</sub> ] .H <sub>2</sub> O [MnC <sub>16</sub> H <sub>16</sub> O <sub>2</sub> N <sub>6</sub> S <sub>2</sub> ].H <sub>2</sub> O	462.94	golden rod	65 %	275 <sup>0</sup> C - 280 <sup>0</sup> C
[Sn (L <sup>1</sup> ) <sub>2</sub> ] [SnC <sub>16</sub> H <sub>16</sub> O <sub>2</sub> N <sub>6</sub> S <sub>2</sub> ]	508.71	greenish yellow	60%	240 <sup>0</sup> C - 250 <sup>0</sup> C
Ligand (L <sup>2</sup> ) C <sub>14</sub> H <sub>11</sub> O <sub>3</sub> N	241	yellow	65 %	241 <sup>0</sup> C - 245 <sup>0</sup> C
[Co(L <sup>2</sup> ) <sub>2</sub> ] .2H <sub>2</sub> O [CoC <sub>28</sub> H <sub>18</sub> O <sub>6</sub> N <sub>2</sub> ].2H <sub>2</sub> O	576.93	golden rod	56 %	above 300 <sup>0</sup> C
Ligand (L <sup>3</sup> ) C <sub>9</sub> H <sub>11</sub> N <sub>3</sub> OS	209	off white	62%	145 <sup>0</sup> C - 150 <sup>0</sup> C
[Cd(L <sup>3</sup> ) <sub>2</sub> ] [CdC <sub>18</sub> H <sub>22</sub> O <sub>2</sub> N <sub>6</sub> S <sub>2</sub> ]	530.41	white	75 %	260 <sup>0</sup> C - 265 <sup>0</sup> C

158

### 159 3.2 Characterizations by Conductivity

160

161 The molar conductivities were obtained using the formula

$$162 \quad \Lambda = \frac{1000}{C} \times \text{Cell constant} \times \text{Observed conductivity.}$$

163 Where,  $\Lambda$ =molar conductance

164 C= concentration

165 The molar conductance is calculated from the measured specific conductance at room  
166 temperature by using the above equation. The experimental results are shown in Table-2.

167

168

169 **Table-2:** Data for the determination of Molar conductivity

Name of Complex	Observed conductivity ( $\text{ohm}^{-1} \text{cm}^2 \text{mol}^{-1}$ )	Molar conductance $\Lambda$ $= (1000/c)$ $\times \text{specificconductance}$ $\text{Scm}^2 \text{mol}^{-1}$	$\mu_{\text{eff}}$ in B.M.	No. of unpaired electron
[Zn (L <sup>1</sup> ) <sub>2</sub> ] .2H <sub>2</sub> O [ZnC <sub>16</sub> H <sub>16</sub> O <sub>2</sub> N <sub>6</sub> S <sub>2</sub> ].2H <sub>2</sub> O	3	3	0.567	–
[Ni (L <sup>1</sup> ) <sub>2</sub> ] .H <sub>2</sub> O [NiC <sub>16</sub> H <sub>16</sub> O <sub>2</sub> N <sub>6</sub> S <sub>2</sub> ].H <sub>2</sub> O	6	6	1.471	–
[Mn (L <sup>1</sup> ) <sub>2</sub> ] .H <sub>2</sub> O [MnC <sub>16</sub> H <sub>16</sub> O <sub>2</sub> N <sub>6</sub> S <sub>2</sub> ].H <sub>2</sub> O	8	8	2.576	1
[Sn (L <sup>1</sup> ) <sub>2</sub> ] [SnC <sub>16</sub> H <sub>16</sub> O <sub>2</sub> N <sub>6</sub> S <sub>2</sub> ]	9	9	0.639	–
[Co(L <sup>2</sup> ) <sub>2</sub> ] .2H <sub>2</sub> O [CoC <sub>28</sub> H <sub>18</sub> O <sub>6</sub> N <sub>2</sub> ].2H <sub>2</sub> O	8	8	4.017	3
[Cd(L <sup>3</sup> ) <sub>2</sub> ] [CdC <sub>18</sub> H <sub>22</sub> O <sub>2</sub> N <sub>6</sub> S <sub>2</sub> ]	6	6	0.461	–

170

171 From the above table data it is showed that all the complexes are non-electrolyte.

172 **3.3 Characterizations by Magnetic Susceptibility**

173 **Measurement of magnetic susceptibility:** The measurements of magnetic susceptibilities  
174 were made at about constant temperature; Curie-law was used and was calculated from the  
175 equation.

$$176 \quad \mu_{\text{eff}} = 2.83 \sqrt{\chi_m^{\text{corr}} \cdot T} \quad \text{B.M.}$$

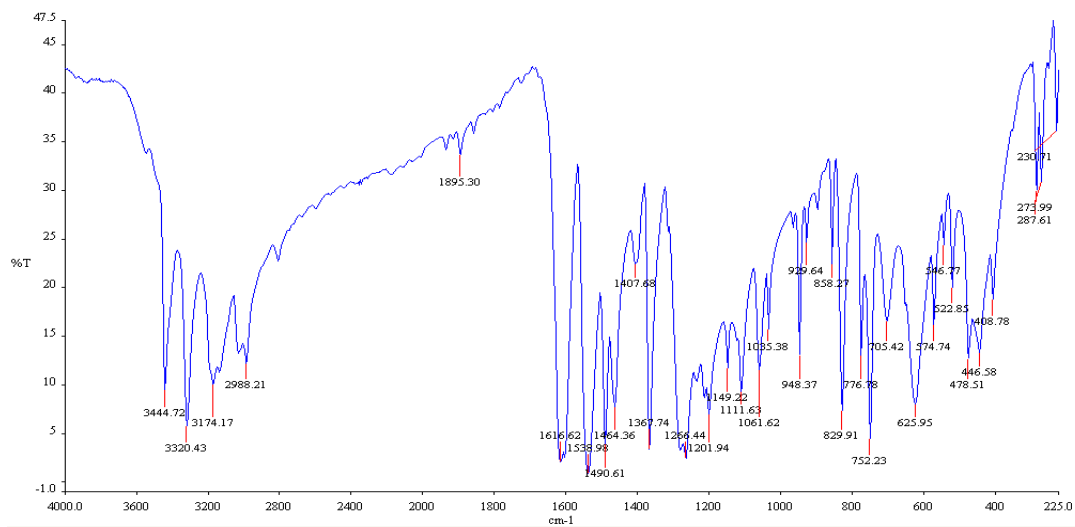
177 Thus  $\mu_{\text{eff}}$  obtained is known as effective magnetic moment. All the values and weight were  
178 expressed in C.G.S. units. The observed values of effective magnetic moment ( $\mu_{\text{eff}}$ ) of the  
179 complexes at room temperature are given in table 2. From the above data it is showed that the  
180 Zn(II), Ni(II), Sn(II) and Cd(II) ions complexes are diamagnetic and Mn(II) and Co(II) ions  
181 complexes are paramagnetic in nature[13].

182 **3.4 Measurement of IR spectra:** At first the complexes heat six hour and KBr overnight in oven.  
 183 Then the complexes and KBr grind with pestle in mortar. Infrared spectra disc were recorded as  
 184 KBr with a NICOLET 310, FTIR spectrophotometer, Belgium, from 4000-225  $\text{cm}^{-1}$ .

### 185 3.4.1 IR spectra of Schiff Base ligand $\text{C}_8\text{H}_9\text{ON}_3\text{S}$ ( $\text{L}^1$ ) and It's metal complexes

#### 186 a. IR spectra of Schiff Base ligand $\text{C}_8\text{H}_9\text{ON}_3\text{S}$ ( $\text{L}^1$ )

187 The spectrum of ligand showed a strong absorption band at  $1616 \text{ cm}^{-1}$  due to the azomethine  
 188  $\nu(\text{C}=\text{N})$  stretching frequency of the free ligand [14-18] indicating that the condensation have  
 189 taken place between the CHO moiety of salicylaldehyde and  $-\text{NH}_2$  moiety of  
 190 thiosemicarbazide. The IR spectra of the free ligand (figure-11) showed two bands at  $3320$   
 191  $\text{cm}^{-1}$  and  $3174 \text{ cm}^{-1}$  may be attributed to the free  $-\text{NH}_2$  and  $\nu(\text{N}-\text{H})$  groups respectively.  
 192 These bands remains in the same region in all complexes spectra, suggesting nonparticipation  
 193 in coordination of one terminal  $-\text{NH}_2$  group in thiosemicarbazone [15,19-21] The band  
 194 observed at  $3444 \text{ cm}^{-1}$  was assigned to the  $\nu(\text{O}-\text{H})$  of hydroxyl group [14,15,22]. The strong  
 195 band  $776 \text{ cm}^{-1}$  for  $\nu(\text{C}=\text{S})$  indicated that  $\text{C}=\text{S}$  bond was present in the Schiff base ligand  
 196 [14,22].



197

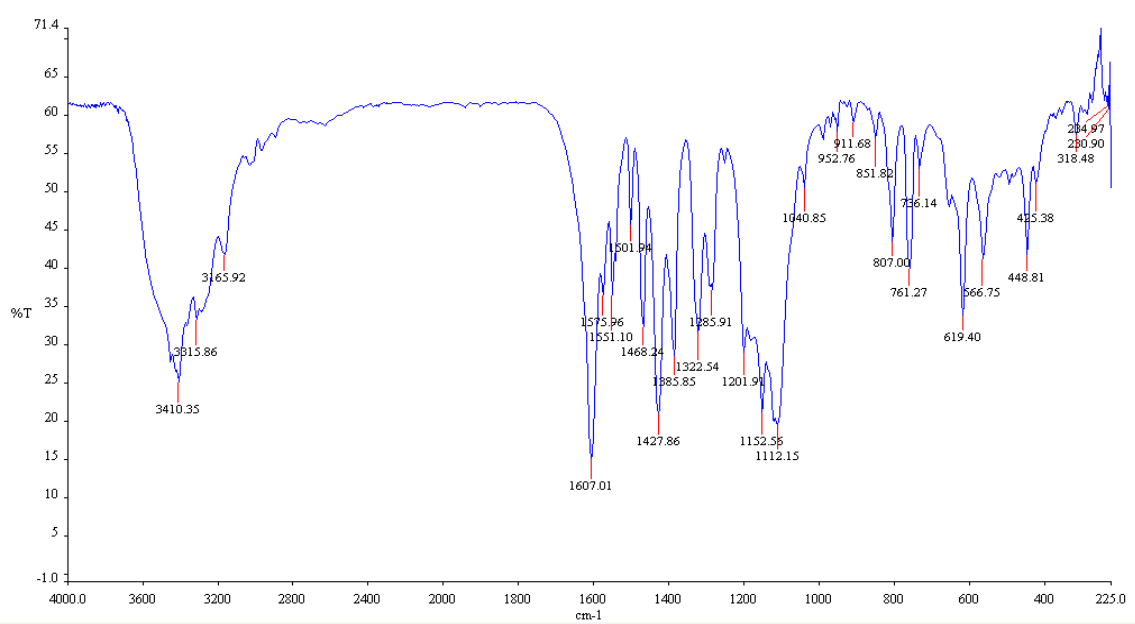
198 Figure-11: IR spectra of Schiff base ligand  $\text{C}_8\text{H}_9\text{ON}_3\text{S}$  ( $\text{L}^1$ )

198

#### 199 b. IR spectra of $[\text{ZnC}_{16}\text{H}_{16}\text{O}_2\text{N}_6\text{S}_2] \cdot 2\text{H}_2\text{O}$ complex

200 In order to determine the mode of coordination of ligand to metal in complexes, IR spectrum  
 201 of ligand was compared with IR spectrum of metal complexes (figure-12). The band at  $1616$   
 202  $\text{cm}^{-1}$  due to the azomethine  $\nu(\text{C}=\text{N})$  stretching frequency of the free ligand that shifted to  
 203 lower frequency in the spectra of the Zn (II) complex at  $1607 \text{ cm}^{-1}$  which indicated the

204 coordination through azomethine N atom. The band  $3444\text{ cm}^{-1}$  due to the  $\nu(\text{O-H})$  of hydroxyl  
 205 group in the IR spectra of the ligand was absent and shifted to lower absorption frequency in  
 206 the IR spectra of Ni(II) complex indicated the coordination through the phenolic oxygen  
 207 [23,24]. This is confirmed by the shift of  $\nu(\text{C-O})$  stretching vibration observed at  $1266\text{ cm}^{-1}$  in  
 208 the spectra of free ligand to  $1285\text{ cm}^{-1}$  stretching vibration of complex after coordination  
 209 [16], which corresponds to forming of weaker C-O(Zn) bond comparing to C-O(H) and  
 210 confirms coordination of ligand to Ni(II) via deprotonated phenolic oxygen [25,26]. Also the  
 211 medium intensity bands observed at  $566\text{ cm}^{-1}$  is attributed to M-O and  $448\text{ cm}^{-1}$  is attributed to  
 212 M-N bonds [27].



213

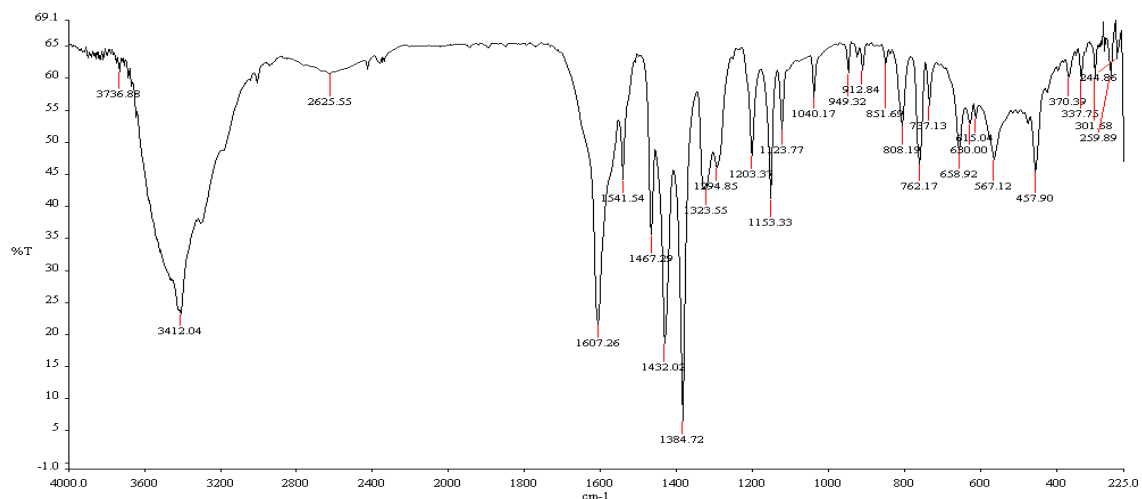
Figure-12: IR spectra of  $[\text{ZnC}_{16}\text{H}_{16}\text{O}_2\text{N}_6\text{S}_2].2\text{H}_2\text{O}$  complex

214

### 215 c. IR spectra of $[\text{NiC}_{16}\text{H}_{16}\text{O}_2\text{N}_6\text{S}_2].\text{H}_2\text{O}$ complex

216 In order to determine the mode of coordination of ligand to metal in complexes IR spectrum  
 217 of ligand was compared with IR spectrum of metal complexes [14, 23]. The band at  $1616\text{ cm}^{-1}$   
 218 <sup>1</sup> due to the azomethine  $\nu(\text{C=N})$  stretching frequency of the free ligand that shifted to lower  
 219 frequency in the spectra of the Ni(II) complex (figure-13) at  $1607\text{ cm}^{-1}$  indicating the  
 220 coordination through N atom [5-9]. The band  $3444\text{ cm}^{-1}$  due to the  $\nu(\text{O-H})$  of hydroxyl  
 221 group in the IR spectra of the ligand was absent and shifted to lower absorption frequency in  
 222 the IR spectra of Ni(II) complex indicated the coordination through the phenolic oxygen  
 223 [22,24]. This is confirmed by the shift of  $\nu(\text{C-O})$  stretching vibration observed at  $1266\text{ cm}^{-1}$   
 224 in the spectra of free ligand to  $1294\text{ cm}^{-1}$  stretching vibration of complex after coordination

225 [16], which corresponds to forming of weaker C-O(Ni) bond comparing to C-O(H) and  
 226 confirms coordination of ligand to Ni(II) via deprotonated phenolic oxygen. Also the medium  
 227 intensity bands observed at  $567\text{ cm}^{-1}$  is attributed to M-O and  $457\text{ cm}^{-1}$  is attributed to M-N  
 228 bonds [27].



229

Figure-13: IR spectra of  $[\text{NiC}_{16}\text{H}_{16}\text{O}_2\text{N}_6\text{S}_2]\cdot\text{H}_2\text{O}$

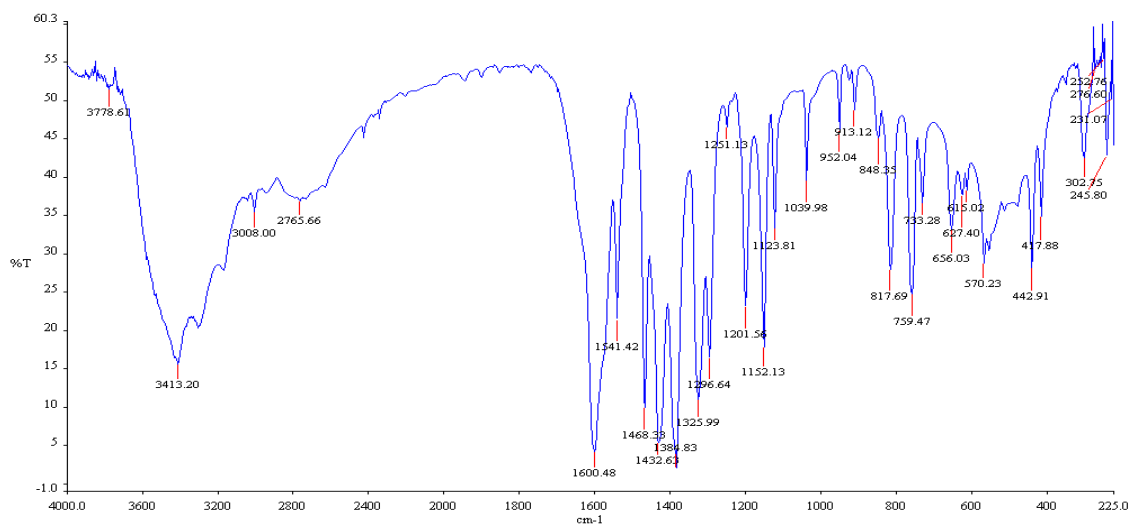
230

#### 231 d. IR spectra of $[\text{MnC}_{16}\text{H}_{16}\text{O}_2\text{N}_6\text{S}_2]$

232 In order to determine the mode of coordination of ligand to metal in complexes IR spectrum  
 233 of ligand was compared with IR spectrum of metal complexes. The band at  $1616\text{ cm}^{-1}$  due to  
 234 the azomethine  $\nu(\text{C}=\text{N})$  stretching frequency of the free ligand that shifted to lower frequency  
 235 in the spectra of the Mn(II) complex (figure-14) at  $1600\text{ cm}^{-1}$  indicating the coordination  
 236 through N atom. The band  $3444\text{ cm}^{-1}$  due to the  $\nu(\text{O}-\text{H})$  of hydroxyl group in the IR spectra  
 237 of the ligand was absent and shifted to lower absorption frequency in the IR spectra of Mn(II)  
 238 complex indicated the coordination through the phenolic oxygen. This is confirmed by the  
 239 shift of  $\nu(\text{C}-\text{O})$  stretching vibration observed at  $1266\text{ cm}^{-1}$  in the spectra of free ligand to  
 240  $1296\text{ cm}^{-1}$  stretching vibration of complex after coordination, which corresponds to forming  
 241 of weaker C-O(Mn) bond comparing to C-O(H) and confirms coordination of ligand to  
 242 Mn(II) via deprotonated phenolic oxygen [5,17]. Also the medium intensity bands observed  
 243 at  $570\text{ cm}^{-1}$  is attributed to M-O and  $442\text{ cm}^{-1}$  is attributed to M-N bonds [27].

244

245



246

247

Figure-14: IR spectra of [MnC<sub>16</sub>H<sub>16</sub>O<sub>2</sub>N<sub>6</sub>S<sub>2</sub>].H<sub>2</sub>O

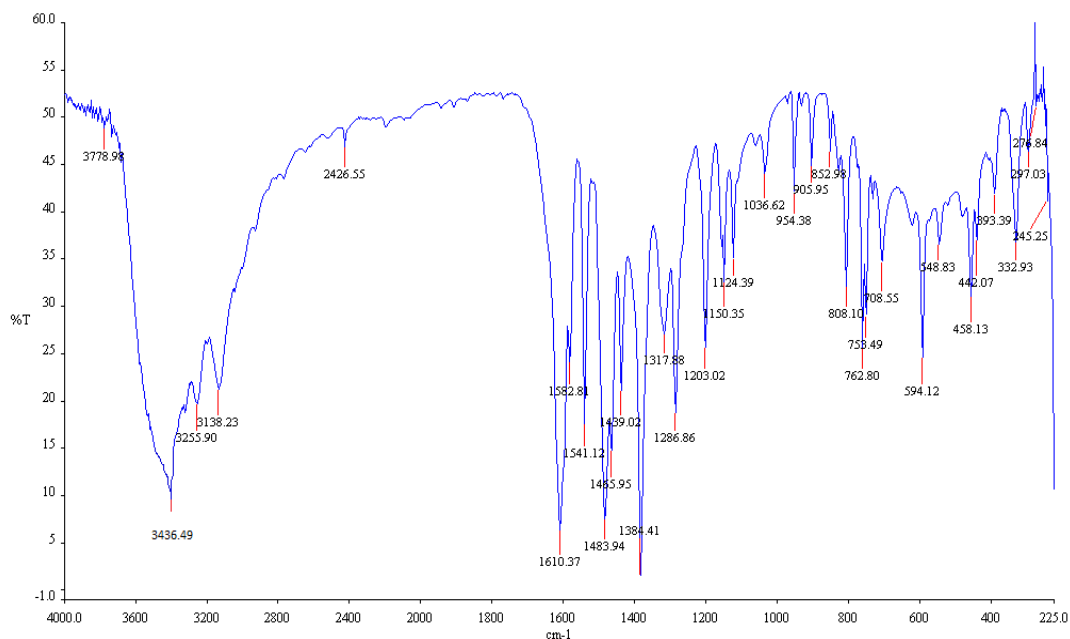
248

**e. IR spectra of [SnC<sub>16</sub>H<sub>16</sub>O<sub>2</sub>N<sub>6</sub>S<sub>2</sub>]**

249

In order to determine the mode of coordination of ligand to metal in complexes IR spectrum of ligand was compared with IR spectrum of metal complexes. The band at 1616 cm<sup>-1</sup> due to the azomethine  $\nu(\text{C}=\text{N})$  stretching frequency of the free ligand that shifted to lower frequency in the spectra of the Sn(II) complex (figure-15) at 1610 cm<sup>-1</sup> indicating the coordination through N atom. The band 3444 cm<sup>-1</sup> due to the  $\nu(\text{O}-\text{H})$  of hydroxyl group in the IR spectra of the ligand was absent and shifted to lower absorption frequency in the IR spectra of Sn(II) complex indicated the coordination through the phenolic oxygen. This is confirmed by the shift of  $\nu(\text{C}-\text{O})$  stretching vibration observed at 1266 cm<sup>-1</sup> in the spectra of free ligand to 1286 cm<sup>-1</sup> stretching vibration of complex after coordination, which corresponds to forming of weaker C-O(Sn) bond comparing to C-O(H) and confirms coordination of ligand to Sn(II) via deprotonated phenolic oxygen. Also the medium intensity bands observed at 594cm<sup>-1</sup> is attributed to M-O and 458cm<sup>-1</sup> is attributed to M-N bonds.

262



263

264

Figure-15: IR spectra of [SnC<sub>16</sub>H<sub>16</sub>O<sub>2</sub>N<sub>6</sub>S<sub>2</sub>]

265

**Table-3:** FTIR spectral data of the ligand C<sub>8</sub>H<sub>9</sub>ON<sub>3</sub>S (L<sup>1</sup>) and it's metal complexes (in cm<sup>-1</sup>)

Ligand / Metal Complexes	IR/cm <sup>-1</sup>				
	ν(O-H)	ν(C=N)	ν(C-O)	ν(M-O)	ν(M-N)
C <sub>8</sub> H <sub>9</sub> ON <sub>3</sub> S	3444	1616	1266	-	-
[ZnC <sub>16</sub> H <sub>16</sub> O <sub>2</sub> N <sub>6</sub> S <sub>2</sub> ].2H <sub>2</sub> O	3410	1607	1285	566	448
[NiC <sub>16</sub> H <sub>16</sub> O <sub>2</sub> N <sub>6</sub> S <sub>2</sub> ].H <sub>2</sub> O	3412	1607	1294	567	457
[MnC <sub>16</sub> H <sub>16</sub> O <sub>2</sub> N <sub>6</sub> S <sub>2</sub> ].H <sub>2</sub> O	3413	1600	1296	570	442
[SnC <sub>16</sub> H <sub>16</sub> O <sub>2</sub> N <sub>6</sub> S <sub>2</sub> ]	3436	1610	1286	594	458

266

267

### 3.4.2 IR spectra of Schiff Base ligand C<sub>14</sub>H<sub>11</sub>O<sub>3</sub>N (L<sup>2</sup>) and It's metal complex

268

#### a. IR spectra of Schiff Base ligand C<sub>14</sub>H<sub>11</sub>O<sub>3</sub>N (L<sup>2</sup>)

269

The bands at 1735 cm<sup>-1</sup> and 3420 cm<sup>-1</sup> due to carbonyl (C=O) and NH<sub>2</sub> stretching vibrations

270

of the starting reagents respectively were absent in the spectra of ligand (figure-16) and a

271

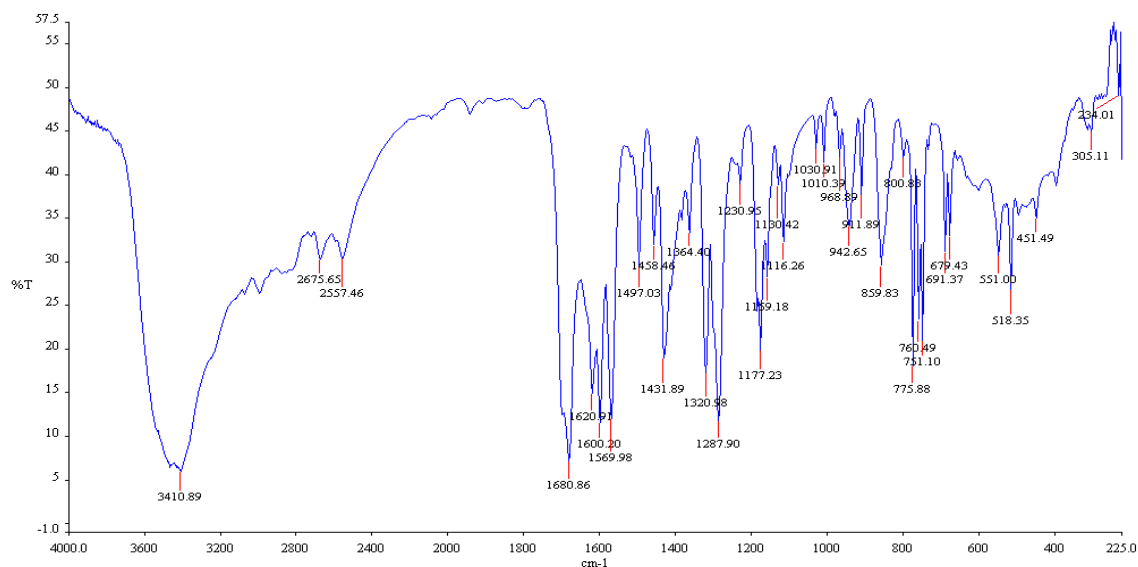
strong new band at 1620 cm<sup>-1</sup> was appeared which assigned to the azomethine (HC=N)

272

linkage, a fundamental feature of Schiff base ligand [28,29]. This indicated that amino and



273 aldehyde moieties of the starting reagents have been converted into the azomethine moiety.  
 274 The bands at  $1320\text{ cm}^{-1}$  due to  $\nu(\text{C-O})$  of phenolic group and  $3410\text{ cm}^{-1}$  due to the phenolic  
 275  $\nu(\text{OH})$  were also observed in the spectra of ligand [23]. The bands at  $1680\text{ cm}^{-1}$  due to  
 276  $\nu(\text{C=O})$  stretching vibration and  $3080\text{ cm}^{-1}$  due to carboxylic  $-\nu(\text{OH})$  were observed in the  
 277 IR spectra of ligand [30-33].



278

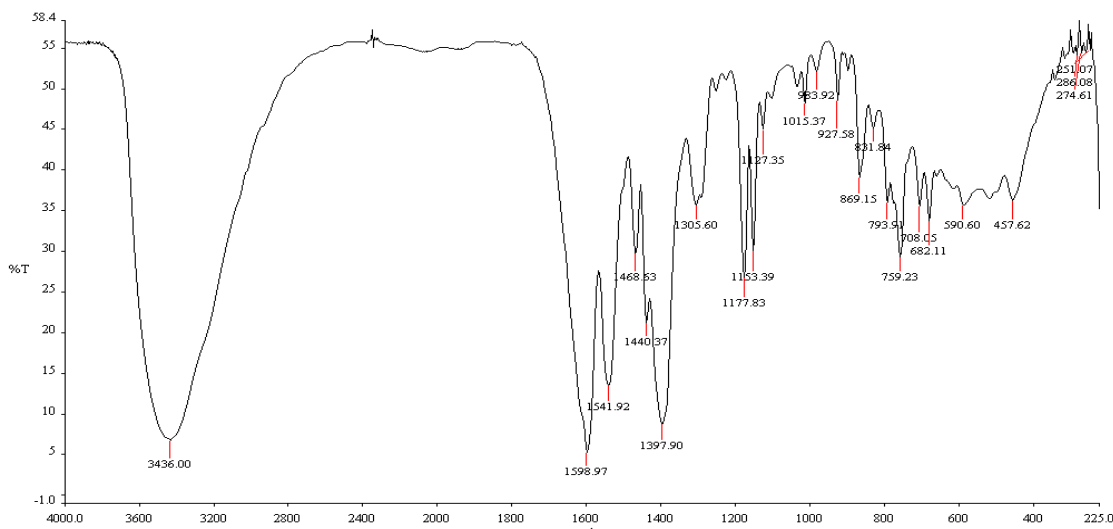
279 Figure-16: IR Spectra of 4-((hydroxybenzylidene)amino)benzoic acid ligand( $L^2$ )

280

### 281 b. IR Spectra of $[\text{CoC}_{28}\text{H}_{18}\text{O}_6\text{N}_2]\cdot 2\text{H}_2\text{O}$

282 The band at  $1620\text{ cm}^{-1}$  due to the azomethine  $-\text{HC}=\text{N}$  stretching vibration was shifted to  
 283 lower frequency at  $1541\text{ cm}^{-1}$  in the metal complex compared to free ligand, suggested the  
 284 coordination of metal ion through nitrogen of azomethine group [34-36]. The N atom of  
 285 azomethine would reduce the electron density in the azomethine link and thus lower the  
 286  $\text{HC}=\text{N}$  absorption after coordination. This is further substantiate by the presence of a new  
 287 band at  $457\text{ cm}^{-1}$  assignable to  $\nu(\text{M-N})$ . The disappearance of phenolic  $\nu(\text{OH})$  band at  $3410$   
 288  $\text{cm}^{-1}$  in  $\text{Co(II)}$  complex suggested the co-ordination by the phenolic oxygen after  
 289 deprotonation to the metal ions. This is further supported by shifting of  $\nu(\text{C-O})$  phenolic  
 290 band at  $1320\text{ cm}^{-1}$  to lower wave number at  $1305\text{ cm}^{-1}$  in the metal complex. The appearance  
 291 of a new band at  $590\text{ cm}^{-1}$  due to  $\nu(\text{M-O})$  in the  $\text{Co(II)}$  complex (figure-17) which further  
 292 substantiate . The band at  $1680\text{ cm}^{-1}$  assigned to  $\nu(\text{C=O})$  in the spectra of ligand also shifted  
 293 to lower frequency range in the metal complex. That suggested the involvement of oxygen  
 294 atom of carboxylic  $\nu(-\text{OH})$  group to the coordination with metal ions. The comparison of the

295 IR spectra of the Schiff base and its metal chelates indicated that the Schiff base ligand  
 296 coordinated to metal ions by three donor atoms representing the ligand acting in a tri-  
 297 dentative manner.



298

Figure-17: IR Spectra of  $[\text{CoC}_{28}\text{H}_{18}\text{O}_6\text{N}_2]\cdot 2\text{H}_2\text{O}$  with ligand ( $\text{L}^2$ )

299

300 **Table-4:** FTIR spectral data of the ligand  $\text{L}^2$  and its Co(II) metal complex (in  $\text{cm}^{-1}$ )

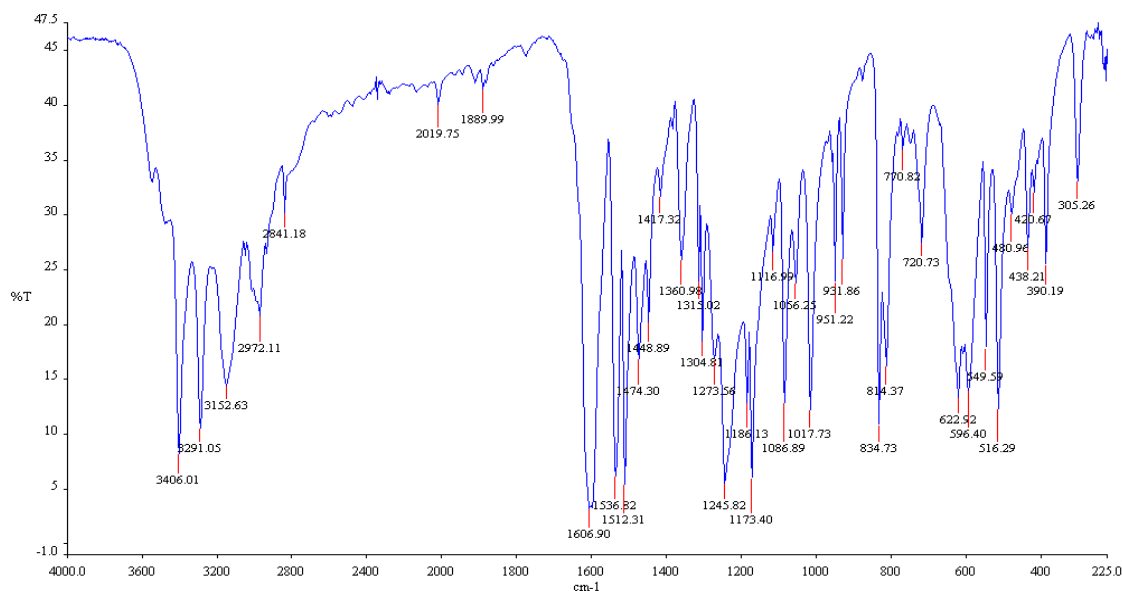
Ligand / Metal Complexes	IR/ $\text{cm}^{-1}$					
	$\nu(\text{O-H})$	$\nu(\text{C=N})$	$\nu(\text{C=O})$	$\nu(\text{C-O})$	$\nu(\text{M-O})$	$\nu(\text{M-N})$
$\text{C}_{14}\text{H}_{11}\text{O}_3\text{N}$	3410	1620	1680	1320	-	-
$[\text{CoC}_{28}\text{H}_{18}\text{O}_6\text{N}_2]\cdot 2\text{H}_2\text{O}$	3436	1541	1598	1305	590	457

301

302 **3.4.3 IR spectra of Schiff Base ligand  $\text{C}_9\text{H}_{11}\text{N}_3\text{OS}$  ( $\text{L}^3$ ) and Its metal complex**

303 **a. IR-Spectra of Schiff base  $\text{C}_9\text{H}_{11}\text{N}_3\text{OS}$  ( $\text{L}^3$ )**

304 The peaks obtained at  $3406\text{cm}^{-1}$  and  $3291\text{cm}^{-1}$  may be assigned to symmetric and asymmetric  
 305  $\nu(-\text{N-H})$  stretching frequency of primary amino group. The broad peak obtained between  
 306  $3282$  and  $2829\text{cm}^{-1}$  may be assigned to overlapping of peaks of hydrogen bonded  $\nu(\text{N-H})$   
 307 and aromatic C-H stretching frequency. The bands obtained between  $1183\text{cm}^{-1}$  and  $1252\text{cm}^{-1}$   
 308  $^1$  in ligand were due to  $\nu(-\text{OCH}_3)$  groups (figure-18). The peaks observed at  $1606\text{cm}^{-1}$  and  $834$   
 309  $\text{cm}^{-1}$  may be assigned to  $\nu(\text{C=N})$  and  $\nu(\text{C=S})$  [37-39].



310

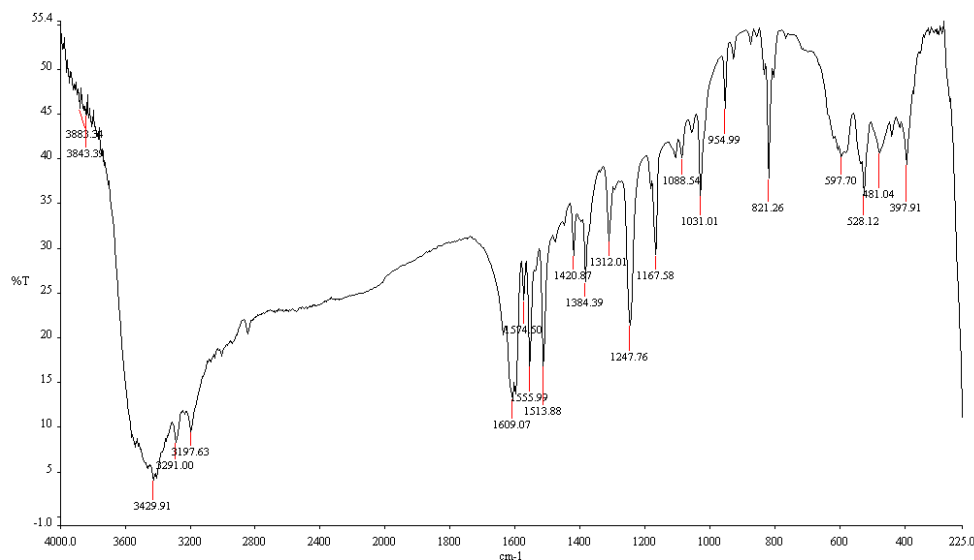
Figure-18: IR Spectra of Schiff base ligand  $C_9H_{11}N_3OS$  ( $L^3$ )

311

312 **b. IR-Spectra of  $[C_{18}H_{22}CdO_2N_6S_2]$  with ligand ( $L^3$ )**

313 The bands at  $1606\text{ cm}^{-1}$  and  $834\text{ cm}^{-1}$  assigned to  $\nu(C=N)$  and  $\nu(C=S)$  modes and these bands  
 314 shifted towards lower frequency in the spectra of Cd(II) complex (figure-19), which indicated  
 315 that coordination takes place through nitrogen of  $\nu(C=N)$  group and sulphur of  $\nu(C=S)$  group.  
 316 At lower frequency the complex exhibited new bands at  $540$  and  $397\text{ cm}^{-1}$  which further  
 317 supported the coordination site  $\nu(M-N)$  and  $\nu(M-S)$  vibrations.

318



319

Figure-19: IR Spectra of  $[CdC_{18}H_{22}O_2N_6S_2]$

320

321 **Table-5:** FTIR spectral data of the ligand  $L^3$  and its Cd(II) metal complex (in  $\text{cm}^{-1}$ )

Ligand / Metal Complexes	IR/ $\text{cm}^{-1}$			
	$\nu(\text{C}=\text{N})$	$\nu(\text{C}=\text{S})$	$\nu(\text{M}-\text{N})$	$\nu(\text{M}-\text{S})$
Ligand ( $L^3$ ) $\text{C}_9\text{H}_{11}\text{N}_3\text{OS}$	1606	834	-	-
$[\text{Cd}(L^3)_2]$ $[\text{CdC}_{18}\text{H}_{22}\text{O}_2\text{N}_6\text{S}_2]$	1574	821	528	397

322

323 **3.5 Characterization by UV-visible Spectra**324 **a. UV-vis spectra and magnetic moment of Zn(II) complex with ligand  $\text{C}_8\text{H}_9\text{ON}_3\text{S}$  ( $L^1$ )**

325 The electronic spectral data for the ligand and their metal complex recorded in DMSO are  
 326 summarized in Table-6. There are two absorption bands, assigned to  $n-\pi^*$  and  $\pi-\pi^*$   
 327 transitions, in the electronic spectrum of the ligand. These transitions are also found in the  
 328 spectra of the complexes, but they are shifted towards lower and higher frequencies,  
 329 indicating the coordination of the ligand to the metallic ions [40]. The UV spectra of the  
 330 ligand shows three absorption bands at 260nm,310nm and 355nm.The first two bands are  
 331 assigned to  $\pi-\pi^*$  transitions of azomethine chromospheres and a benzene ring and the third is  
 332 assigned to  $n-\pi^*$  transition of a lone pair of electrons of an azomethine nitrogen and an  
 333 antibonding  $\pi$  orbital. The absorption band  $n-\pi^*$ at 355 nm due to an imine group in the  
 334 ligand, whereas for the zinc complex, the same was observed at 390 nm with weak absorption  
 335 intensity which indicate the coordination of zinc with imine group [41]. The zinc complex  
 336 shows only the charge transfer transition which can be assigned to charge transfer from the  
 337 ligand to the metal and vice versa, no d-d transitions are expected for  $d^{10}\text{Zn(II)}$  complex [42].

338 **b. UV-vis spectra and magnetic moment of Ni(II) complex with ligand  $\text{C}_8\text{H}_9\text{ON}_3\text{S}$  ( $L^1$ )**

339 The UV-Vis absorption spectra of the ligand and complex were recorded after dissolving into  
 340 DMSO solvent at room temperature. There are two absorption bands, assigned to  $n-\pi^*$  and  
 341  $\pi-\pi^*$  transitions, in the electronic spectrum of the ligand. These transitions are also found in  
 342 the spectra of the complexes, but they are shifted towards lower and higher frequencies,  
 343 confirming the coordination of the ligand to the metallic ions [43]. The electronic spectrum of  
 344 ligand exhibits three intense absorption peaks at 260 nm, 310 nm and 350nm.The first and  
 345 second peaks were attributed to benzene  $\pi-\pi^*$ and imino  $\pi-\pi^*$ transitions and the third peak in

346 the spectra was assigned to  $n-\pi^*$  transition [44]. The electronic spectra of the Ni(II) complex  
347 with an electronic configuration of  $d^8$  shows three new absorption bands in the visible region  
348 and these three bands of the transitions  $^1A_{1g} \rightarrow ^1A_{2g}$  (355nm),  $^1A_{1g} \rightarrow ^1B_{1g}$  (380nm) and  
349  $^1A_{1g} \rightarrow ^1E_g$  (420 nm) were observed in the spectra of a square-planar Ni(II) complex [45,46].

350 **c. UV-vis spectra and magnetic moment of Mn(II) complex with ligand  $C_8H_9ON_3S$  ( $L^1$ )**

351 The UV-Vis absorption spectra of the ligand and complex were recorded after dissolving into  
352 DMSO solvent at room temperature. There are two absorption bands, assigned to  $n-\pi^*$  and  
353  $\pi-\pi^*$  transitions, in the electronic spectrum of the ligand. These transitions are also found in  
354 the spectra of the complexes, but the ligand to the metallic ions [47]. The electronic spectrum  
355 of ligand exhibits three intense absorption peaks at 260 nm, 310 nm and 350nm. The first and  
356 second peaks were attributed to benzene  $\pi-\pi^*$  and imino  $\pi-\pi^*$  transitions and the third peak in  
357 the spectra was assigned to  $n-\pi^*$  transition. Due to Forbidden transition, several bands were  
358 observed in the visible region of Mn(II) complex, and the band at 430 nm is attributed to (d-  
359 d) transition of type  $^6A_1 \rightarrow ^4T_2$ .

360 **d. UV-vis spectra and magnetic moment of Sn(II) complex with ligand  $C_8H_9ON_3S$  ( $L^1$ )**

361 The electronic absorption spectra of ligand  $L^1$  and its Sn (II) complex in DMSO solution  
362 were carried out in the range of 200-800 nm at room temperature. There is a shift of the  
363 bands to longer wave length in spectra of complex is a good evidence of complex formation.  
364 There were various bands in the ligand spectra assigned to inter ligand and charge transfer of  
365  $n-\pi^*$  transitions according to their energies and intensities. Ligand exhibits three intense  
366 absorption peaks at 260 nm, 310 nm and 350nm. The first and second peaks were attributed to  
367 benzene  $\pi-\pi^*$  and imino  $\pi-\pi^*$  transitions and the third band in the spectra was assigned to  $n-$   
368  $\pi^*$  transition. The complex showed an intense band at 410nm due to the  $n-\pi^*$  transition of  
369 azomethine chromosphere and the band at 340 nm may be assigned as charge transfer band. It  
370 has been reported that the metal is capable of forming  $dn-p\pi^*$  bonds with ligands containing  
371 nitrogen as the donor atom. The Sn atom has its 5d orbital completely vacant and hence  
372  $Sn \leftarrow N$  bonding can take place by the acceptance of the lone pair of electrons from the  
373 azomethine nitrogen of the ligand [48-50].

374

375

376 **Table-6:** Magnetic moments and electronic spectral data for ligand ( $L^1$ ) and its metal  
 377 complexes

Compound	$\lambda_{\max}$ n.m	Wave number $\text{cm}^{-1}$	$\mu_{\text{eff}}$ B.M	Assignment
$\text{C}_8\text{H}_9\text{ON}_3\text{S}$	260	38461	-	$\pi \rightarrow \pi^*$
	310	32258		$\pi \rightarrow \pi^*$
	350	38571		$n \rightarrow \pi^*$
$[\text{NiC}_{16}\text{H}_{16}\text{O}_2\text{N}_6\text{S}_2] \cdot \text{H}_2\text{O}$	355	28169	1.469	${}^1\text{A}_{1g} \rightarrow {}^1\text{A}_{2g}$
	380	26315		${}^1\text{A}_{1g} \rightarrow {}^1\text{B}_{1g}$
	420	23809		${}^1\text{A}_{1g} \rightarrow {}^1\text{E}_g$
$[\text{ZnC}_{16}\text{H}_{16}\text{O}_2\text{N}_6\text{S}_2] \cdot 2\text{H}_2\text{O}$	265	37735	0.5197	C.T ( $\text{M} \rightarrow \text{L}$ )
	320	31250		C.T ( $\text{M} \rightarrow \text{L}$ )
	390	25641		C.T ( $\text{M} \rightarrow \text{L}$ )
$[\text{MnC}_{16}\text{H}_{16}\text{O}_2\text{N}_6\text{S}_2] \cdot \text{H}_2\text{O}$	325	30769	2.507	${}^6\text{A}_1 \rightarrow {}^4\text{T}_2$
	380	26315		
	430	23255		

378

379 **e. UV-vis spectra and magnetic moment of Co(II) complex with ligand  $\text{C}_{14}\text{H}_{11}\text{O}_3\text{N}$  ( $L^2$ )**

380 The magnetic moment and electronic spectra are very effective in the evaluation of results  
 381 obtained by other methods of structural investigation. Information regarding the geometry of  
 382 the complex of Co(II) ions was obtained from electronic spectral studies and magnetic  
 383 moments (table-7). The electronic spectra of ligand and their metal complexes were recorded  
 384 in DMSO. Electronic spectrum of ligand shows strong absorption band at 330nm region can  
 385 be assigned to the  $n \rightarrow \pi^*$  transition of the azomethine group of ligand, which slightly shifted  
 386 to lower frequency in the spectra of the complex, indicating that the azomethine nitrogen  
 387 atom is involved in coordination to the metal ion. The Co(II) complex was found the  
 388 magnetic moment 4.0137 B.M which indicated the three unpaired electrons per Co(II) ion  
 389 attaining an octahedral environment [60]. The electronic spectrum of Co(II) complex shows  
 390 bands at 264nm and 274nm are assignable to metal-ligand charge transfer band and the band  
 391 400nm is assignable to  ${}^4\text{T}_{1g}(\text{F}) \rightarrow {}^4\text{T}_{1g}(\text{P})$  transition.

392

393 **Table-7:** The electronic spectral data and magnetic moments for ligand ( $L^2$ ) and it's metal  
 394 complex

Compound	$\lambda_{\max}$ n.m	Wave number $\text{cm}^{-1}$	$\mu_{\text{eff}}$ B.M	Assignment
$\text{C}_{14}\text{H}_{11}\text{O}_3\text{N}$	330	30303	-	$n \rightarrow \pi^*$
$[\text{CoC}_{28}\text{H}_{18}\text{O}_6\text{N}_2] \cdot 2\text{H}_2\text{O}$	264	37878	4.0137	Charge transfer(C.T)
	274	36496		C.T ( $M \rightarrow L$ )
	400	25000		${}^4T_{1g}(F) \rightarrow {}^4T_{1g}(P)$

395

396 **f. UV-vis spectra and magnetic moment of Cd(II) complex with ligand  $\text{C}_9\text{H}_{11}\text{N}_3\text{OS}$  ( $L^3$ )**

397 The electronic spectral data for the ligand and it's metal complex recorded in DMSO are  
 398 summarized in Table-8. There are two absorption bands, assigned to  $n-\pi^*$  and  $\pi-\pi^*$   
 399 transitions, in the electronic spectrum of the ligand. These transitions are also found in the  
 400 spectra of the complexes, but they are shifted towards lower and higher frequencies,  
 401 indicating the coordination of the ligand to the metallic ions. The UV spectra of the ligand  
 402 shows three absorption bands at 280nm,330nm and 350nm.The first two bands are assigned  
 403 to  $\pi-\pi^*$  transitions of azomethine chromospheres and a benzene ring and the third is assigned  
 404 to  $n-\pi^*$  transition of a lone pair of electrons of an azomethine nitrogen and an anti-bonding  $\pi$   
 405 orbital. The absorption band  $n-\pi^*$  at 350nm due to an imine group in the ligand, whereas for  
 406 the Cd(II) complex, the same was observed at 400 nm with weak absorption intensity which  
 407 indicate the coordination of cadmium with imine group. The cadmium complex show only  
 408 the charge transfer transition which can be assigned to charge transfer from the ligand to the  
 409 metal and vice versa, no d-d transition are expected for diamagnetic  $d^{10}$  Cd(II) complex. The  
 410 shifting of ligand absorption in the UV region, in the spectra of the complex confirming the  
 411 coordination of the ligand to metal like Cd (II) ions.

412

413

414

415

416 **Table-8:** Magnetic moments and electronic spectral data for ligand ( $L^3$ ) and it's Cd(II)  
 417 Complex

Compound	$\lambda_{\max}$ n.m	Wave number $\text{cm}^{-1}$	$\mu_{\text{eff}}$ B.M	Assignment
$\text{C}_9\text{H}_{11}\text{N}_3\text{OS}$	280	35714	-	$\pi \rightarrow \pi^*$
	330	30303		$\pi \rightarrow \pi^*$
	350	28571		$n \rightarrow \pi^*$
$[\text{CdC}_{18}\text{H}_{22}\text{O}_2\text{N}_6\text{S}_2]$	295	33898	0.4606	C.T (M $\rightarrow$ L)
	340	29412		C.T (M $\rightarrow$ L)
	400	25000		C.T (M $\rightarrow$ L)

418

### 419 3.6 Characterization by Thermogravimetric Analysis

#### 420 Thermogravimetric analysis of Zn(II),Ni(II),Mn(II) and Sn(II) complexes of ligand 421 $\text{C}_8\text{H}_9\text{ON}_3\text{S}$ ( $L^1$ )

422 The thermal decomposition analysis of solid Zn(II), Ni(II), Mn(II) and Sn(II) metal  
 423 complexes were carried out under nitrogen atmosphere and heating rate was suitably  
 424 controlled at  $30^\circ\text{C min}^{-1}$  and the weight loss was measured from the ambient temperature up  
 425 to  $800^\circ\text{C}$ .The data from TGA and DTG clearly indicated that the decomposition of the  
 426 complexes proceed in three or four steps. There were some minor steps and asymmetry of  
 427 TGA/DTG curves also observed. The weight losses for each complex were calculated within  
 428 the corresponding temperature ranges. The different thermodynamic parameters are listed in  
 429 Table-9.

#### 430 a. For $[\text{ZnC}_{16}\text{H}_{16}\text{O}_2\text{N}_6\text{S}_2].2\text{H}_2\text{O}$ Complex

431 The TGA and DTG curve of Zn(II) complex shown in (figure-20), indicated that the complex  
 432 was decomposed into four main steps. In the first step of decomposition, two molecules of  
 433 water were lost at the temperature range of  $85\text{-}110^\circ\text{C}$  (calculated 7.36%, experimental  
 434 7.20%). In this temperature range the loss of water molecules indicates that the water  
 435 molecules are of lattice type [51,52].In the temperature range  $130\text{-}335^\circ\text{C}$  (calculated 24.00%  
 436 and experimental 23.10%), the part of ligand- $2\text{CSNH}_2$  were decomposed at the second step.  
 437 The other part of the ligand  $2\text{C}_6\text{H}_4\text{O}$ - were decomposed in third step at  $335\text{-}740^\circ\text{C}$  (calculated  
 438 37.50%, experimental 32 .00%). At above  $750^\circ\text{C}$  temperature the complex was decomposed



439 and removed as Zn/ZnO (calculated 31.14%, experimental 37.70%) polluted with few carbon  
440 atoms [53].

441 **b. For  $[\text{NiC}_{16}\text{H}_{16}\text{O}_2\text{N}_6\text{S}_2]\cdot\text{H}_2\text{O}$  Complex**

442 The TGA and DTG curve of Ni(II) complex shown in (figure-21) that the complex was  
443 decomposed into four main steps. The 1<sup>st</sup> step involves the removal of one molecule of  
444 hydrated water (calculated 3.87%, experimental 4.00% weight) at temperature range 80-  
445 190°C [54,55]. In the 2<sup>nd</sup> step the part of the ligand  $2\text{C}_6\text{H}_4\text{O}^-$  was decomposed at 280-350°C  
446 (calculated 39.59%, experimental 34.82% weight). At the 3<sup>rd</sup> step the fragmentation of  
447 coordinated ligand  $2\text{C}_2\text{H}_4\text{N}_3\text{S}$  was decomposed from the complex at the temperature range  
448 360-750°C (calculated 43.90%, experimental 44.20% weight) and above 750°C temperature  
449 the complex was completely decomposed and removed as Ni/NiO (calculated 12.64%,  
450 experimental 16.98%).

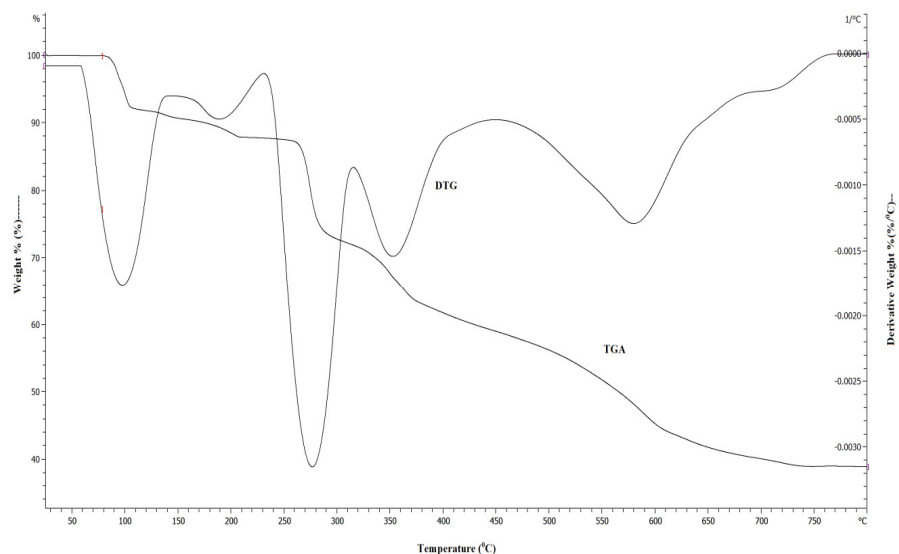
451 **c. For  $[\text{MnC}_{16}\text{H}_{16}\text{O}_2\text{N}_6\text{S}_2]\cdot\text{H}_2\text{O}$  Complex**

452 In the case of Mn(II) complex the TGA and DTG curve indicated in (figure-22) that the  
453 complex was decomposed into four main steps. At 1<sup>st</sup> step one molecule of hydrated water  
454 was removed at 80-180°C (calculated 3.90%, experimental 4.00%) [54,55]. Then the  
455 dehydrated complex was gradually decomposed and the part of ligand  $2\text{C}_6\text{H}_4\text{O}^-$  was removed  
456 at the temperature range 180-350°C (calculated 39.92%, experimental 38.10%). The 3<sup>rd</sup> step  
457 involves the decomposition of the ligand part  $2\text{CH}_3\text{N}_2\text{S}$  at the temperature range 350-  
458 770°C (calculated 32.54%, experimental 32.22%). At above 770°C temperature finally the  
459 complex was completely decomposed and removed as Mn/MnO (calculated 23.64%,  
460 experimental 25.68%).

461 **d. For  $[\text{SnC}_{16}\text{H}_{16}\text{O}_2\text{N}_6\text{S}_2]$  Complex**

462 The Sn(II) complex showed high thermal stability and decomposed above 170 °C, indicating  
463 the absence of any lattice water molecules[69]. This complex was decomposed into four main  
464 steps shown in (figure-23). At first step the part of ligand  $(-2\text{CH}_2\text{NS})$  were decomposed  
465 at temperature 170-275°C (calculated 23.67%, experimental 22.00%). In 2<sup>nd</sup> step the  
466 decomposition of  $(-2\text{CHN}-)$  moiety was take place at temperature 275-330°C (calculated  
467 12.0%, experimental 10.65 %). The ligand part  $(2\text{C}_6\text{H}_4\text{O}^-)$  were decomposed at the 3<sup>rd</sup> step at  
468 temperature range 330-750°C (calculated 36.29%, experimental 36.10 %) and finally the

469 complex was completely decomposed and removed as Sn/SnO (calculated 28.04%,  
 470 experimental 31.25%).

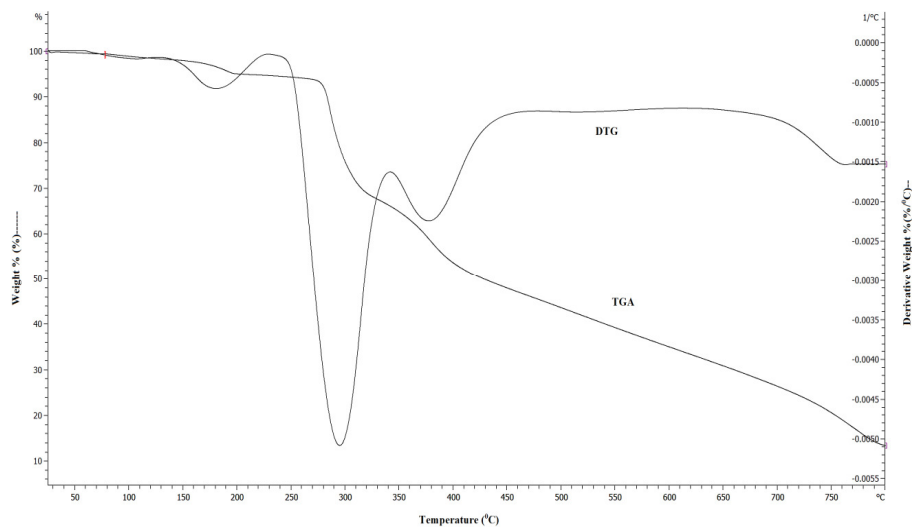


471

472 Figure-20: TGA and DTG curve of  $[ZnC_{16}H_{16}O_2N_6S_2] \cdot 2H_2O$

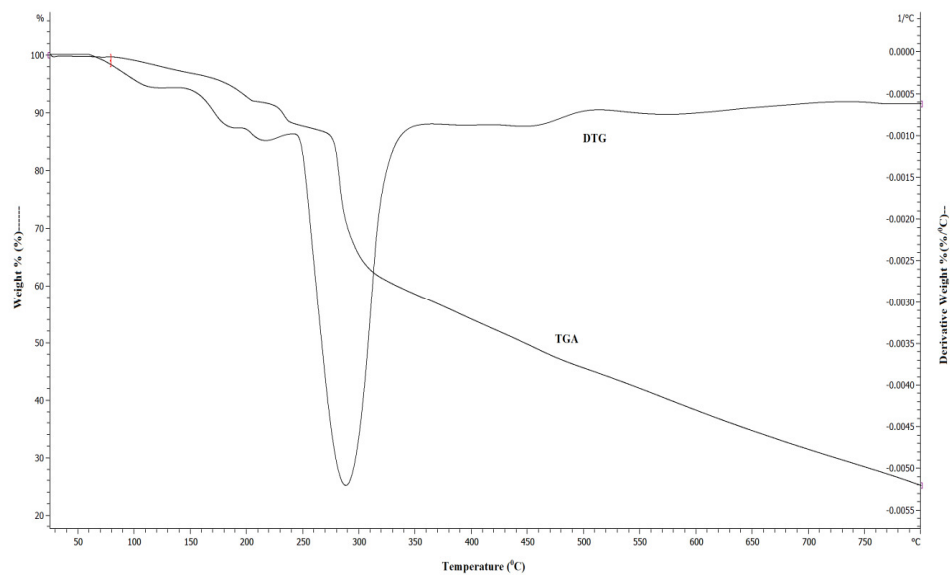
473

474



475

476 Figure-21: TGA and DTG curve of  $[NiC_{16}H_{16}O_2N_6S_2] \cdot H_2O$

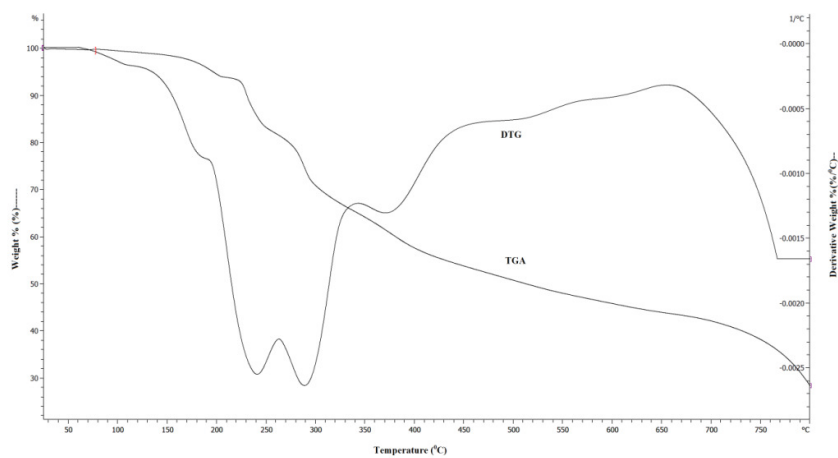


477

478

Figure-22: TGA and DTG curve of  $[MnC_{16}H_{16}O_2N_6S_2].H_2O$

479



480

481

Figure-23: TGA and DTG curve of  $[SnC_{16}H_{16}O_2N_6S_2]$

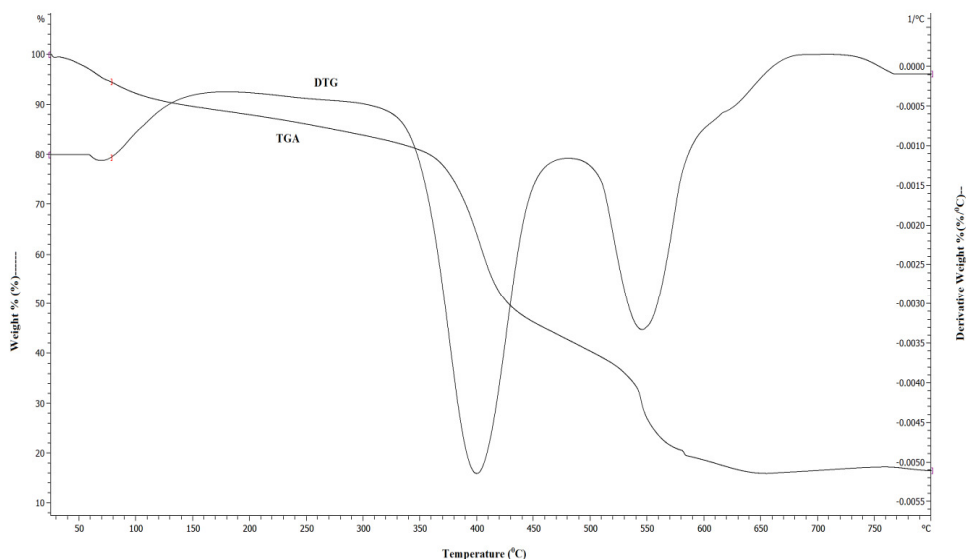
482 **Table- 9:** Thermal data of Zn(II), Ni(II), Mn(II) and Sn(II) complexes of ligand  $C_8H_9ON_3S$   
 483 ( $L^1$ )

Complexes	Steps	Temperature Range/ °C	DTG Peak/ °C	TG mass loss% calc./found	Assignments
-----------	-------	-----------------------	--------------	---------------------------	-------------

[ZnC <sub>16</sub> H <sub>16</sub> O <sub>2</sub> N <sub>6</sub> S <sub>2</sub> ].2H <sub>2</sub> O	1 <sup>st</sup>	85-110	97	7.36/7.20	2H <sub>2</sub> O
	2 <sup>nd</sup>	130-335	278	24.00/23.10	2CSNH <sub>2</sub>
	3 <sup>rd</sup>	335-740	350	37.50/32.00	2C <sub>6</sub> H <sub>4</sub> O-
	4 <sup>th</sup>	>750		31.14/37.7	Zn/ZnO
[NiC <sub>16</sub> H <sub>16</sub> O <sub>2</sub> N <sub>6</sub> S <sub>2</sub> ].H <sub>2</sub> O	1 <sup>st</sup>	80-190	180	3.87/4.00	H <sub>2</sub> O
	2 <sup>nd</sup>	280-350	295	39.59/34.82	2C <sub>6</sub> H <sub>4</sub> O <sup>-</sup>
	3 <sup>rd</sup>	360-750	382	43.90/44.20	2C <sub>2</sub> H <sub>4</sub> N <sub>3</sub> S
	4 <sup>th</sup>	>750		12.64/16.98	Ni/NiO
[MnC <sub>16</sub> H <sub>16</sub> O <sub>2</sub> N <sub>6</sub> S <sub>2</sub> ].H <sub>2</sub> O	1 <sup>st</sup>	80-180	118	3.90/4.00	H <sub>2</sub> O
	2 <sup>nd</sup>	180-350	290	39.92/38.10	2C <sub>6</sub> H <sub>4</sub> O <sup>-</sup>
	3 <sup>rd</sup>	350-770		32.54/32.22	2CH <sub>3</sub> N <sub>2</sub> S
	4 <sup>th</sup>	>770		23.64/25.68	Mn/MnO
[SnC <sub>16</sub> H <sub>16</sub> O <sub>2</sub> N <sub>6</sub> S <sub>2</sub> ]	1 <sup>st</sup>	170-275	240	23.67/22.00	2CH <sub>2</sub> NS
	2 <sup>nd</sup>	275-330	290	12.00/10.65	2CHN-
	3 <sup>rd</sup>	330-750	370	36.29/36.10	2C <sub>6</sub> H <sub>4</sub> O <sup>-</sup>
	4 <sup>th</sup>	>750		28.04/31.25	Sn/SnO

484 **Thermogravimetric analysis of Co(II) complex of ligand C<sub>14</sub>H<sub>11</sub>O<sub>3</sub>N (L<sup>2</sup>)**

485 TGA was carried out for solid Co(II) metal complex under N<sub>2</sub> flow. The heating rate was  
486 suitably controlled at 30°C min<sup>-1</sup> and the weight loss was measured from the ambient  
487 temperature up to 800°C. The thermogram of complex exhibits three clear cut decomposition  
488 stages in (figure-24). The first stage with estimated mass loss of 6.32% (calculated mass loss  
489 6.28%) within the temperature range 40–110°C corresponding to the loss of water molecules  
490 [56,57]. The second stage occurs at 110–480°C, with a mass loss of 49.20% (calculated  
491 51.31%) , corresponding to the loss of 2C<sub>8</sub>H<sub>5</sub>O<sub>2</sub>N parts of the ligand. The third stage of  
492 decomposition occurs at the temperature range 480–650°C, with a mass loss of 28.80%  
493 (calculated 32.12%), corresponding to the loss of 2C<sub>6</sub>H<sub>4</sub>O moiety. At above 650°C  
494 temperature the complex was completely decomposed and removed as of 15.72% (calculated  
495 10.29%). The different TG and DTG data are given in Table-10.



496

497

Figure-24: TGA and DTG curve of  $[\text{CoC}_{28}\text{H}_{18}\text{O}_6\text{N}_2]\cdot 2\text{H}_2\text{O}$

498

**Table- 10:** Thermal data of Co(II) complex of ligand  $\text{C}_{14}\text{H}_{11}\text{O}_3\text{N}$  ( $\text{L}^2$ )

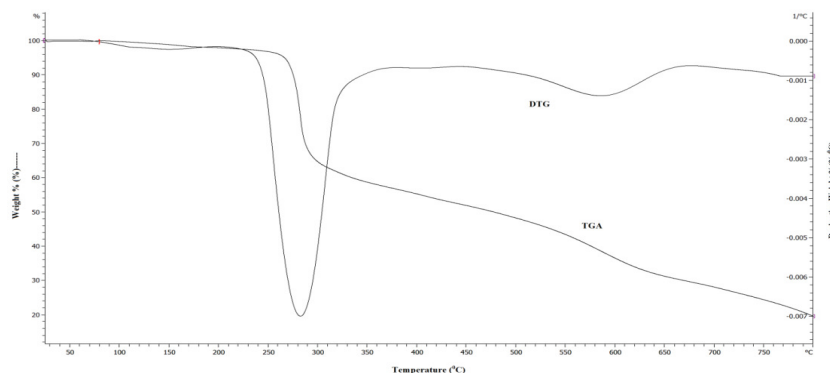
Complexes	Steps	Temperature Range/ °C	DTG Peak/ °C	TG mass loss% calc./found	Assignments
$[\text{CoC}_{28}\text{H}_{18}\text{O}_6\text{N}_2]\cdot 2\text{H}_2\text{O}$	1 <sup>st</sup>	40-110	65	6.28/6.32	$2\text{H}_2\text{O}$
	2 <sup>nd</sup>	110-480	400	51.31/49.20	$2\text{C}_8\text{H}_5\text{O}_2\text{N}$
	3 <sup>rd</sup>	480-650	548	32.12/28.80	$2\text{C}_6\text{H}_4\text{O}$
	4 <sup>th</sup>	>650		10.29/15.72	Co/CoO

499

500 **Thermogravimetric analysis of Cd(II) complex of ligand  $\text{C}_9\text{H}_{11}\text{N}_3\text{OS}$  ( $\text{L}^3$ )**

501 Thermogravimetric analysis of solid Cd(II) metal complex under  $\text{N}_2$  flow. The heating rate  
 502 was suitably controlled at  $30^\circ\text{C min}^{-1}$  and the weight loss was measured from the ambient  
 503 temperature up to  $800^\circ\text{C}$ . The TGA curve of the Cd(II) complex showed no mass loss up to  
 504  $230^\circ\text{C}$ , indicating the absence of lattice / coordinated water [58,59] and the high thermal  
 505 stability of the complex. The thermogram of Cd(II) complex is given in Fig.4.24, which  
 506 shows two stage decomposition pattern. The first stage was exhibited a maximum mass loss  
 507 of 49.23% (calculated 50.53%) of ligand part ( $2\text{C}_8\text{H}_8\text{ON}$ ) at  $230\text{--}455^\circ\text{C}$ . The second stage  
 508 occurs at  $455\text{--}740^\circ\text{C}$ , with a mass loss of 27.05% (calculated 28.28%) attributed to the loss  
 509 of ( $2\text{CH}_3\text{N}_2\text{S}$ ) moiety. Finally at above  $750^\circ\text{C}$  temperature the complex was completely

510 decomposed and removed as Cd/CdO of 24.0% (calculated 21.19%). The different TG and  
 511 DTG data are given in Table-11.



512

513 Figure-25: TGA and DTG curve of  $[CdC_{18}H_{22}O_2N_6S_2]$

513

514 **Table- 11:** Thermal data of Cd(II) complex of ligand  $C_9H_{11}N_3OS (L^3)$

Complexes	Steps	Temperature Range/ °C	DTG Peak/ °C	TG mass loss% calc./found	Assignments
$[CdC_{18}H_{22}O_2N_6S_2]$	1 <sup>st</sup>	230-455	282	50.53/49.23	$2C_8H_8ON$
	2 <sup>nd</sup>	455-740	570	28.28/27.05	$2CH_3N_2S$
	3 <sup>rd</sup>	>740		21.19/24.00	Cd/CdO

515

516 **Antibacterial activity**

517 The prime objective of performing the antibacterial screening is to determine the  
 518 susceptibility of the pathogenic microorganism to test the compound which, in turn is used to  
 519 selection of the compound as a therapeutic agent. The free Schiff base ligand and their metal  
 520 complexes were screened for their antibacterial activity against strains the *Bacillus cereus*  
 521 *ATCC25923*, *Streptococcus agelactiae*, *Escherichia coli ATCC 25922*, *Shigella dysenteriae*  
 522 The compounds were tested at a concentration of 30  $\mu$ g/0.01 mL in DMSO solution using the  
 523 paper disc diffusion method with Kanamycin as standard. The susceptibility zones were  
 524 measured in diameter (mm) and the result are listed in Table-12. The susceptibility zones  
 525 were the clear zones around the discs killing the bacteria.

526

527

528 **Table 12.** Antibacterial activities of the complexes.

Bacterials strains	Zone of inhibition, diameter in mm						
	A (10µg /disc)	B (10µg /disc)	C (10µg /disc)	D (10µg /disc)	E (10µg /disc)	F (10µg /disc)	K (30µg /disc)
<b>Gram positive</b>							
<i>Bacillus cereus</i>	22	10	19	12	11	14	36
<i>Streptococcus agelactiae</i>	19	09	21	08	14	16	35
<b>Gram negative</b>							
<i>Escherichia coli</i>	23	12	24	09	12	18	32
<i>Shigella dysenteriae</i>	09	11	10	12	08	14	36

529

530 Where, A =  $[C_{16}H_{16}ZnO_2N_6S_2].2H_2O$ , B =  $[C_{16}H_{16}NiO_2N_6S_2].H_2O$ , C =  $[C_{16}H_{16}MnO_2N_6S_2].H_2O$ , D =  
 531  $[C_{16}H_{16}SnO_2N_6S_2]$ , E =  $[C_{28}H_{18}CoO_6N_2].2H_2O$ , F =  $[C_{18}H_{22}CdO_2N_6S_2]$  and K = Kanamycin

532 **Conclusion**

533 In this paper we have explored the synthesis and coordination Chemistry of Ni(II), Zn(II),  
 534 Mn(II), Sn(II), Co(II) and Cd(II) ions were synthesized with three different synthesized  
 535 Schiff base ligands viz (L<sup>1</sup>) [2-(2-hydroxybenzylidene)hydrazinecarbothioamide], (L<sup>2</sup>) [4-((4-  
 536 hydroxybenzylidene)amino)benzoic acid and (L<sup>3</sup>) [2-(4-  
 537 methoxybenzylidene)hydrazinecarbothioamide]. The ligands and metal complexes were  
 538 characterized by molar conductivity measurement, magnetic susceptibility, Infrared,  
 539 electronic spectral, thermal analysis and some physical measurements. The overall reactions  
 540 were monitored by TLC analysis. Molar conductance study have shown that all the  
 541 complexes were non electrolytic in nature. FTIR studies suggested that Schiff bases act as  
 542 deprotonated bidentate ligands and metal ions are attached with the ligands-(L<sup>1</sup>), (L<sup>2</sup>) by N, O

543 and ligand-(L<sup>3</sup>) by N, S coordinating sites during complexation reaction. Magnetic  
544 susceptibility data coupled with electronic spectra revealed that [ZnC<sub>16</sub>H<sub>16</sub>O<sub>2</sub>N<sub>6</sub>S<sub>2</sub>].2H<sub>2</sub>O,  
545 [MnC<sub>16</sub>H<sub>16</sub>O<sub>2</sub>N<sub>6</sub>S<sub>2</sub>].H<sub>2</sub>O, [SnC<sub>16</sub>H<sub>16</sub>O<sub>2</sub>N<sub>6</sub>S<sub>2</sub>] and [CdC<sub>18</sub>H<sub>22</sub>O<sub>2</sub>N<sub>6</sub>S<sub>2</sub>] complexes have tetrahedral,  
546 [NiC<sub>16</sub>H<sub>16</sub>O<sub>2</sub>N<sub>6</sub>S<sub>2</sub>].H<sub>2</sub>O has square planer and [CoC<sub>28</sub>H<sub>18</sub>O<sub>6</sub>N<sub>2</sub>].2H<sub>2</sub>O has octahedral geometry.  
547 Thermal analysis (TGA and DTG) data showed the possible degradation pathway of the  
548 complexes and also indicated that most of the complexes were thermally stable up to 200<sup>0</sup>C.  
549 The Schiff bases and their metal complexes have been found moderate to strong  
550 antimicrobial activity.

#### 551 REFERENCES

- 552 [1]. Angela Kriza, Lucica Viorica Ababei, Nicoleta Cioatera, Ileana Rău And Nicolae  
553 Stănică, Synthesis And Structural Studies Of Complexes Of Cu, Co, Ni And Zn With  
554 Isonicotinic Acid Hydrazide And Isonicotinic Acid (1-Naphthylmethylene)Hydrazide,  
555 J. Serb. Chem. Soc., 2010,75 (2), 229- 242.
- 556 [2]. P. K. Das, N. Panda, N. K. Behera, Synthesis, Characterization and Antimicrobial  
557 Activities of Schiff Base Complexes Derived from Isoniazid and Diacetylmonoxime,  
558 IJISSET - International Journal of Innovative Science, Engineering & Technology,  
559 2016, 3( 1).
- 560 [3]. Anil Kumar M R, Shanmukhappa S, Rangaswamy B E, Revanasiddappa M,  
561 Synthesis, Characterization, Antimicrobial Activity, Antifungal Activity and DNA  
562 Cleavage Studies of Transition Metal Complexes with Schiff Base Ligand,  
563 International Journal of Innovative Research in Science, Engineering and Technology,  
564 2015,4( 2).
- 565 [4]. O' Boyle N M, Tenderholt A L & Langer K M, cclib: a library for package-  
566 independent computational chemistry algorithms J. Comput. Chem., 2008, 29, 839.
- 567 [5]. Spectromica Acta Part A , 2012, 93, 86-94.
- 568 [6]. K.D. Karlin, Z. Tyeklar, Bioinorganic Chemistry of Copper, Chapman & Hall: New  
569 York, 1993, 101-109.
- 570 [7]. V. Arun, N. Sridevi, P.P. Robinson, S. Manju, K.K.M. Yusuff, "Ni(II) and Ru(II)  
571 Schiff base complexes as catalysts for the reduction of benzene" J. Mol. Catal. A:  
572 Chem., 2009, 304 (1-2), 191-198.
- 573 [8]. K. C. Gupta, A. K. Sutar, Catalytic activities of Schiff base transition metal  
574 complexes, Coord. Chem. Rev., 2008, 252, 1420.



- 575 [9]. R. I. Kureshy, N. H. Khan, S. H. R. Abdi, P. Iyer and S. T. Patel ,Chiral Ru(II) Schiff  
576 base complexes catalysed enantio selective epoxidation of styrene derivatives using  
577 iodosyl benzene as oxidant II, *J. Mol. Catal.*, 1999,150,150.
- 578 [10]. Saud I. Al-Resayes, Mohammad Shakirb, Ambreen Abbasi, Kr. Mohammad Yusuf  
579 Amin, Abdul Lateef, *Spectromica Act.a Part A*, 2012, 93, 86-94.
- 580 [11]. Rakesh Ranjan and Dhanashree S Hallooman, Synthesis And Characterization Of  
581 Co(Ii) And Ni(Ii) Complexes With Schiff Base 2,2-  
582 Dimethylpropioiphenonethiosemicarbazone, *International Journal Of Research In*  
583 *Pharmacy And Chemistry*, 2014, 4(2), 423-426.
- 584 [12]. Angela Kriza, Mariana Loredana Dianu, Nicolae Stănică, Constantin Drăghici, Mona  
585 Popoiu, Synthesis and Characterization of Some Transition Metals Complexes with  
586 Glyoxalbis- Isonicotinoyl Hydrazone, 2009, 60(6).
- 587 [13]. 4. L. Mitu, A. Kriza, Synthesis and Characterization of Complexes of Mn(II),  
588 Co(II), Ni(II) and Cu(II) with an Aroylhydrazone Ligand. *Asian J. Chem.*, 2007, 19  
589 (1), 658-664.
- 590 [14]. Ljubijankić N., Tešević V., Grgurić-Šipka S., Jadranin M., Begić S., Buljubašić L.,  
591 Markotić E., Ljubijankić S., Synthesis and characterization of Ru(III) complexes with  
592 thiosemicarbazide-based ligands, 2016, 47, 1-6.
- 593 [15]. Methak. S. Mohammad, Preparation and Characterization of Some Transition Metal  
594 Complexes withSchiff base of thiosemicarbazone, *Journal of Kerbala University,*  
595 *Scientific*. 2010, 8 (1).
- 596 [16]. R.V. Singh, N. Fahmi and M.K. Biyala, Coordination Behavior and Biopotency of N  
597 and S/O Donor Ligands with their Palladium(II) and Platinum(II) Complexes, *Journal*  
598 *of the Iranian Chemical Society*, 2005, 2(1), 40-46.
- 599 [17]. A. M. Vijey, G. Shiny, and V. Vaidhyalingam, Synthesis and antimicrobial activities  
600 of 1-(5-substituted-2-oxo indolin-3-ylidene)-4-(substituted pyridin-2-yl)  
601 thiosemicarbazide, *Arkivoc (xi)*., 2008, 187.
- 602 [18]. Mohammad Asif, A Review On Biological Activities Of Benzimidazole, Oxadiazole  
603 And Mannich Base Derivatives Of Benzimidazole-Oxadiazole Merged Compounds,  
604 *International Journal of Current Research in Applied Chemistry & Chemical*  
605 *Engineering*, 2017, 3(1).
- 606 [19]. M. M. H. Khalil, M. M. Aboaly and R. M. Ramadan, Spectroscopic and  
607 electrochemical studies of ruthenium and osmium complexes of salicylideneimine-2-  
608 thiophenol Schiff base, 2005, 61(1), 157-161.

- 609 [20]. 11. P. M. Dahikar, R. M. Kedar, Synthesis, spectral and biological activity of  
610 transition metal complexes of substituted benzoinsemicarbazones, International  
611 Journal of Application or Innovation in Engineering & Management (IJAIEM), 2013,  
612 2(4).
- 613 [21]. P. Murali Krishna, B. S. Shankara, and N. Shashidhar Reddy, Synthesis,  
614 Characterization, and Biological Studies of Binuclear Copper(II) Complexes of (2E)-  
615 2-(2-Hydroxy-3-Methoxybenzylidene)-4N-Substituted Hydrazine carbothioamides,  
616 Hindawi Publishing Corporation, International Journal of Inorganic Chemistry,  
617 2013, 11 pages.
- 618 [22]. Ljiljana S. Vojinović-Ješić, Vukadin M. Leovac, Mirjana M. Lalović, Valerija I.  
619 Češljević, Ljiljana S. Jovanović, Marko V. Rodić and Vladimir Divjaković, Transition  
620 metal complexes with thiosemicarbazide-based ligands. Part 58. Synthesis, spectral  
621 and structural characterization of dioxovanadium(V) complexes with  
622 salicylaldehydethiosemicarbazone, J. Serb. Chem. Soc. 2011, 76 (6), 865–877.
- 623 [23]. Monika Tyagi, Sulekh Chandra, Synthesis, characterization and biocidal properties of  
624 platinum metal complexes derived from 2,6-diacetylpyridine (bisthiosemicarbazone),  
625 Open Journal of Inorganic Chemistry, 2012, 2, 41-48.
- 626 [24]. Vojinović-Ješić Lj. S., Leovac V.M., Lalović M. M., Češljević V.I., Jovanović  
627 Lj.S. Rodić M. V. and Divjaković V, Transition metal complexes with  
628 thiosemicarbazide-based ligands. Part 58. Synthesis, spectral and structural  
629 characterization of dioxovanadium(V) complexes with salicyl aldehyde  
630 thiosemicarbazone, J. Serb. Chem. Soc., 2011, 76 (6), 865–877.
- 631 [25]. Baiu S.H., El-Ajaily M.M. and El-Barasi, Antibacterial Activity of Schiff Base  
632 Chelates of Divalent Metal Ions, Asian Journal of Chemistry, (2009), 21(1), 5-10.
- 633 [26]. Elena Pahontu, Valeriu Fala, Aurelian Gulea, Donald Poirier, Victor Tapcov and  
634 Tudor Rosu, Synthesis and Characterization of Some New Cu(II), Ni(II) and Zn(II)  
635 Complexes with Salicylidene Thiosemicarbazones: Antibacterial, Antifungal and in  
636 Vitro Antileukemia Activity, Molecules, 2013, 18, 8812-8836.
- 637 [27]. El-Bahnasawy R. M., Sharaf El-Deen L.M., El-Table A.S., Wahba M. A. and El-  
638 Monsef. A., Electrical Conductivity Of Salicylaldehyde Thiosemicarbazone and its  
639 Pd(II), Cu(II) and Ru(III) Complexes, Eur. Chem. Bull, 2014, 3(5), 441-446.
- 640 [28]. Md. Saddam Hossain, C.M. Zakaria, M.M. Haque, and Md. Kudrat-E-Zahan, Spectral  
641 and thermal characterization with antimicrobial activity on Cr(III) and Sn(II)

- 642           Complexes containing N,O Donor novel schiff base ligand, International Journal of  
643           Chemical Studies,2016, 4(6), 08-11.
- 644   [29]. A. Xavier, P. Gopu ,B. Akila,K. Suganya, Synthesis and Characterization of Schiff  
645           Base from 3, 5-Di ChloroSalicylaldehyde with 4-Bromoaniline and 4-Aminobenzoic  
646           Acid and Its 1st Row Transition Metal Complexes, International Journal Of  
647           Innovative Research & Development, 2015, 4( 8).
- 648   [30]. 22.    Manohar V. Lokhande and Mrityunjay R. Choudhary, Some Transitional  
649           Metal Ions Complexes With 3-{[(E)-(4-Fluorophenyl) Methylidene] Amino} Benzoic  
650           Acid And Its Microbial Activity, International Journal of Pharmaceutical Sciences  
651           and Research, IJPSR, 2014, 5(5), 1757-1766.
- 652   [31]. P. Gopu, Dr. A. Xavier,Synthesis and Characterization of 4-(3-bromo-5 -chloro-2-  
653           hydroxybenzlidimino) Benzoic Acid and its Transition Metal Complexes,  
654           International Journal of Science and Research (IJSR), 2015, 4,(8).
- 655   [32]. Shanker K, Rohini R, Ravinder V and Reddy P M: Ru(II) complexes of N<sub>4</sub> and N<sub>2</sub>O<sub>2</sub>  
656           macrocyclic Schiff base ligands: Their antibacterial and antifungal studies, Spectro  
657           chimica Acta A, 2009, 73, 1205-211.
- 658   [33]. Raju Ashokan, Saravanan Sathishkumar, Ekamparam Akila And Rangappan Rajavel,  
659           Synthesis, Characterization and Biological Activity of Schiff Base Metal Complexes  
660           Derived from 2, 4-Dihydroxyactophenone, Chemical Science Transactions , 2017,  
661           6(2), 277-287 .
- 662   [34]. Miguel-Angel Munoz-Hernandes, Michal L. Mckee, Timothy S. Keizer, Burt C.  
663           Yearwood and David Atwood, Six-coordinate aluminiumcations: characterization,  
664           catalysis, and theory, 2002,3.
- 665   [35]. K. Nakamoto: Infrared Spectra of Inorganic and Coordination Compounds. John  
666           Wiley & Sons, New York, 2nd Edition, 1970.
- 667   [36]. Shanker K B, Rohini M, Ravinder Reddy P and Ho M Y P: Synthesis of Tetraaza  
668           Macrocyclic Pd(II) complexes; Antibacterial & Catalytic studies, J.of the Ind. Chem.  
669           Soc. 2009, 86.
- 670   [37]. K.P. Satheesh, V. Suryanarayana Rao, Spectrophotometric Method For The  
671           Determination Of Trace Amount Of Tungsten (Vi) In Alloy Samples Using 4-  
672           Hydroxybenzaldehydethiosemicarbazon, Journal of Advanced Scientific Research,  
673           2015, 6(2), 14-17.

- 674 [38]. S. Janarthanan, Y.C. Rajan, P.R. Umarani, D. Jayaraman, D. Premanand and S. Pandi,  
675 Synthesis, growth, optical and thermal properties of a new organic crystal  
676 semicarbazone of p-anisaldehyde, (SPAS), 2010, 3(8).
- 677 [39]. Ruchi Agarwal, Mohd. Asif Khan and Shamim Ahmad, Schiff base complexes  
678 derived from thiosemicarbazone, synthesis characterization and their biological  
679 activity , Journal of Chemical and Pharmaceutical Research, 2013, 5(10), 240-245.
- 680 [40]. Sandra S. Konstantinovi, Blaga C. Radovanovi, IvojinCaki And VesnaVasi, Synthesis  
681 and characterization of Co(II), Ni(II), Cu(II) and Zn(II) complexes with 3-  
682 salicylidenehydrazono-2-indolinone,J.Serb.Chem.Soc., 2003, 68(8-9), 641-647.
- 683 [41]. N. K. Gondia, J. Priya, S. K. Sharma, Synthesis and physico-chemical  
684 characterization of a Schiff base and its zinc complex, Res Chem Intermed, 2017,  
685 43,1165-1178.
- 686 [42]. Lotf A. Saghatforoush, Ali Aminkhani, Sohrab Ershad, Ghasem Karimnezhad,  
687 Shahriar Ghammamy and Roya Kabiri, Preparation of Zinc (II) and Cadmium (II)  
688 Complexes of the Tetradentate Schiff Base Ligand 2-((E)-(2-(2(pyridine-2-yl)-  
689 ethylthio)ethylimino)methyl)-4-bromophenol (PytBrsalH), Molecules 2008, 13, 804-  
690 811.
- 691 [43]. Jian-Ning Liu, Bo-Wan Wu, Bing Zhang, Yongchun Liu, Synthesis and  
692 Characterization of Metal Complexes of Cu(II), Ni(II), Zn(II), Co(II), Mn(II) and  
693 Cd(II) with Tetradentate Schiff Bases, Turk J Chem., 2006,30 , 41-48.
- 694 [44]. Shayma A. Shaker, Preparation and Spectral Properties of Mixed-Ligand Complexes  
695 of VO(IV), Ni(II), Zn(II), Pd(II), Cd(II) and Pb(II) with Dimethylglyoxime and N-  
696 Acetyl glycine, E-Journal of Chemistry, 2010, 7(S1), S580-S586.
- 697 [45]. Md. Kudrat-E-Zahan, M. S. Islam, and Md. Abul Bashar ,Synthesis, Characteristics,  
698 and Antimicrobial Activity of Some Complexes of Mn(II), Fe(III) Co(II), Ni(II),  
699 Cu(II), and Sb(III) Containing Bidentate Schiff Base of SMDTC, Russian Journal of  
700 General Chemistry, 2015,85(3),667-672.
- 701 [46]. Rehab K. Al-Shemary, Ahmed T. Numanand Eman Mutar Atiyah, Synthesis,  
702 Characterization And Antimicrobial Evaluation Of Mixed Ligand Complexes Of  
703 Manganese(Ii), Cobalt(Ii), Copper(Ii), Nickel(Ii) And Mercury(Ii) With 1,10-  
704 Phenanthroline And A Bidentate Schiff Base, Eur. Chem. Bull., 2016, 5(8), 335-338.
- 705 [47]. Iniyama, G.E., Olarele, O.S. and Johnson, A, Synthesis, spectral, characterization and  
706 antimicrobial activity of manganese (II) and copper (II) complexes of

- 707 Salicylaldehydephenylhydrazone, International Journal of Chemistry and  
708 Applications, 2015, 7(1), 15-23.
- 709 [48]. Neelofar, Nauman Ali, Shabir Ahmad, Naser M. Abdel-Salam, Riaz Ullah, Robila  
710 Nawaz and Sohail Ahmad, Synthesis and evaluation of antioxidant and antimicrobial  
711 activities of Schiff base tin (II) complexes, Tropical Journal of Pharmaceutical  
712 Research ,2016,15(12), 2693-2700.
- 713 [49]. Har Lal Singh and J. B. Singh, Synthesis and Characterization of New Lead(II)and  
714 Organotin(IV) Complexes of Schiff Bases Derived from Histidine and Methionine,  
715 Hindawi Publishing Corporation, International Journal of Inorganic Chemistry,  
716 2012,7pages.
- 717 [50]. Sunita Bhanuka and Har Lal Singh, Spectral, Dft And Antibacterial Studies Of Tin(Ii)  
718 Complexes Of Schiff Bases Derived From Aromatic Aldehyde And Amino Acids,  
719 Rasayan J. Chem., 2017, 10(2), 673-68.
- 720 [51]. Khalil Abid, Sinann Al-Bayati, Anaam Rasheed, Synthesis, Characterization,  
721 Thermal study and Biological Evaluation of Transition Metal Complexes Supported  
722 by ONNNO-Pentadentate Schiff Base Ligand, American Journal of Chemistry, 2016,  
723 6(1), 1-7.
- 724 [52]. Allan J. R. and Veitch P. M., (1983) J. Thermal Anal., 27,P3.
- 725 [53]. Moamen S. Refat, I. M. El-Deen, M. S. El-Garib, and W. Abd El-Fattah,  
726 Spectroscopic and Anticancer Studies on New Synthesized Copper(II) and  
727 Manganese(II) Complexes with 1,2,4- Triazines Thiosemicarbazide1, Russian Journal  
728 of General Chemistry, 2015, 85( 3), 692–707.
- 729 [54]. Md. Saddam Hossain, Md. Ashraful Islam, C. M. Zakaria, M. M. Haque, Md. Abdul  
730 Mannan, Md. Kudrat-E-Zahan, Synthesis, Spectral and Thermal Characterization with  
731 Antimicrobial Studies on Mn(II), Fe(II), Co(II) and Sn(II) Complexes of Tridentate  
732 N,O Coordinating Novel Schiff Base Ligand” J. Chem. Bio. Phy. Sci. Sec. A., 2016,6  
733 (1),041-052.
- 734 [55]. M. R. Islam, J. A. Shampa, M. Kudrat-E-Zahan, M. M. Haque, Y. Reza, Investigation  
735 on Spectroscopic, Thermal and Antimicrobial Activity of Newly Synthesized  
736 Binuclear Cr(III) Metal Ion Complex , J. Sci. Res., 2016, 8 (2), 181-189.
- 737 [56]. Sayed M. Abdallah, M.A. Zayed, Gehad G. Mohamed, Synthesis and spectroscopic  
738 characterization of new tetradentate Schiff base and its coordination compounds of  
739 NOON donor atoms and their antibacterial and antifungal activity, Arabian Journal of  
740 Chemistry, 2010, 3, 103–113.

- 741 [57]. Samir Alghool. Mononuclear complexes based on reduced Schiff base derived fromL-  
742 methionine, synthesis, characterization, thermal and in vitro antimicrobial studies, J  
743 Therm Anal Calorim, 2015, 12, 1309–1319.
- 744 [58]. Achut S. Munde, Amarnath N. Jagdale, Sarika M. Jadhav And Trimbak K.  
745 Chondhekar, Synthesis, characterization and thermal study of some transition metal  
746 complexes of an asymmetrical tetradentate Schiff base ligand, J. Serb. Chem. Soc.,  
747 2010, 75(3),349–359.
- 748 [59]. A.S. Munde, V. A. Shelke, S. M. Jadhav, A. S. Kirdant, S. R. Vaidya, S. G.  
749 Shankarwar, and T. K. Chondhekar, Synthesis, Characterization and Antimicrobial  
750 Activities of some Transition Metal Complexes of Biologically Active Asymmetrical  
751 Tetradentate Ligands, Adv. Appl. Sci. Res., 2012, 3(1),175-182.